On the Analysis of an Optimization Approach to Slow Manifold Computation in Chemical Kinetics

Diploma Thesis

submitted by

Jonas Unger

Advisors:

PD Dr. Dirk Lebiedz
Prof. Dr. Dietmar Kröner

Freiburg, August 2010

Albert-Ludwigs-Universität Freiburg
Fakultät für Mathematik und Physik

Erklärung

Hiermit erkläre ich, dass ich diese Arbeit selbstständig verfasst, keine anderen als die angegebenen Quellen und Hilfsmittel benutzt und alle Stellen, die dem Wortlaut oder Sinne nach anderen Werken entnommen sind, durch Angabe der Quellen als Entlehnung kenntlich gemacht habe.

Freiburg, 5. August 2010

(Jonas Unger)

Contents

Acknowledgment

I want to thank

- Dirk Lebiedz for giving me the opportunity to write my diploma thesis in his working group. His ideas and knowledge have made this work possible. Thank you for the very good supervision during the last year!
- Dietmar Kröner for supervising my diploma thesis and for helpful suggestions.
- Jochen Siehr for having so much patience with me. Thank you for helping me with my diploma thesis!
- Mario Mommer for the fruitful discussions with my supervisor Dirk Lebiedz which led to important aspects concerning my diploma thesis.
- the whole working group: Dominik Skanda, Jochen Siehr, Kai Antweiler, Marc Fein, Marcel Rehberg, Markus Esenwein, and Melanie Franzem.
- all people who have proofread this thesis.
- my whole family for supporting me the whole time and making my studies possible.
- my girlfriend Deborah for always being by my side. I also want to thank her family.
- all my friends for having a nice time while I have been writing my diploma thesis.

Chapter 1

Introduction

1.1 Motivation

Chemically reactive flows play a key role in a broad range of technical combustion applications. The mathematical modeling of those reactive flows is very complex because they include an interplay between *flow (convection)*, *diffusive transport*, and *chemical combustion reaction processes*. The simulation of these processes – based on a detailed combustion mechanism involving a large number of chemical species and reactions – is up to now difficult despite growing computing power. However, detailed knowledge and numerical simulations of chemical combustion – which plays a major role for the use of energy (amongst others) in today's world – are necessary and call for complexity reduction and multi-scale approaches.

A common feature of the chemical kinetics model equations (*Ordinary Differential Equations (ODEs)* $\dot{c}(t) = f\left(c(t)\right),\ c(t) \in \mathbb{R}^n$) corresponding to a complex model (chemical reaction mechanism) is the occurence of a large number of different time scales. In order to simplify these stiff model equations, model reduction techniques have to be applied for obtaining a reduced model. Many model reduction methods exploit this time scale separation into fast and slow modes with the aim of approximating the system dynamics with a dimension-reduced model via eliminating the fast modes by enslaving them to the slow ones. Therefore, most model reduction techniques make use of the occurence within the phase space of a *Slow Invariant attracting Manifold (SIM)*, which attracts nearby orbits and possesses a lower dimensionality than the phase space. These SIMs are characterized by their properties, which are *invariance* and *attractivity*. The dynamics on such SIMs govern the long term evolution of the full model. Nearby orbits decompose into a fast component that contracts toward the SIM and a slow component obeying the system dynamics on the SIM. Thus, the aim of these model reduction approaches is the identification and approximation of such SIMs.

These slow manifolds are parameterized by so-called *reaction progress variables*, which are typically slow variables (i.e. variables, that represent the slow modes of the system). For the computation of SIMs a *species reconstruction* technique is used in this work (not later than here it has to be mentioned, that SIMs are present in the phase space of the dynamical systems considered in this work). Species reconstruction represents a function mapping such reaction progress variables onto the full species composition by determining a point on the SIM. In this sense, the fast variables (i.e. variables, that represent the fast modes of the system) become slaved to the reaction progress variables.

1.2 Different Model Reduction Methods

Model reduction methods for ODE modeling chemical kinetics have been developed for about one hundred years. Most methods make use of the occurence within the phase space of a SIM which attracts nearby orbits and possesses a lower dimensionality than the phase space. The high-dimensional dynamical systems, which describe the corresponding processes, often involve multiple time scales and because of this stiffness, many model reduction methods assume singularly perturbed systems for analysis of the technique with a singular perturbation parameter measuring time scale separation.

Five model reduction methods are exemplarily mentioned here. First, two basic approaches are listed followed by three modern model reduction methods developed during the last ten years. The three modern approaches are chosen according to their close relation to the here presented model reduction method.

Among the first model reduction methods in chemical kinetics have been the *Quasi Steady-State Assumption (QSSA)* [5, 6, 7] and the *Partial Equilibrium Assumption (PEA)* [30]. In the QSSA approach certain species are assumed to be in steady-state whereas in the PEA approach certain reactions are assumed to be in equilibrium.

The right hand side of some of the differential equations describing the chemical mechanism is set to zero in the QSSA method. Example:

$$\begin{aligned}
\frac{\mathrm{d}[\mathrm{S}_1]}{\mathrm{d}t} &= -k_{12}[\mathrm{S}_1] \\
\frac{\mathrm{d}[\mathrm{S}_2]}{\mathrm{d}t} &= k_{12}[\mathrm{S}_1] - k_{23}[\mathrm{S}_2] = 0 \\
\frac{\mathrm{d}[\mathrm{S}_3]}{\mathrm{d}t} &= k_{23}[\mathrm{S}_2].
\end{aligned}$$

This means that the rates of change of some species depend on the rates of change of the other species:

$$[\mathrm{S}_2] = \frac{k_{12}}{k_{23}}[\mathrm{S}_1].$$

Thus, certain ODEs can be replaced by algebraic equations such that the original ODE system changes to a differential algebraic equation system:

$$\begin{aligned}\frac{\mathrm{d}[\mathrm{S}_1]}{\mathrm{d}t} &= -k_{12}[\mathrm{S}_1] \\ [\mathrm{S}_2] &= \frac{k_{12}}{k_{23}}[\mathrm{S}_1] \\ \frac{\mathrm{d}[\mathrm{S}_3]}{\mathrm{d}t} &= k_{23}[\mathrm{S}_2].\end{aligned}$$

Finally, the number of differential variables has been reduced (from $[\mathrm{S}_1]$, $[\mathrm{S}_2]$, $[\mathrm{S}_3]$ to $[\mathrm{S}_1]$, $[\mathrm{S}_3]$).

In contrast to the QSSA approach where the major assumption is on species, in the PEA approach the major assumption is on reactions. The latter assumes fast elementary reaction steps to be relaxed to partial equilibrium immediately.

Both methods require a detailed knowledge of the mechanism in order to decide for which species a quasi-stationarity or for which reactions a partial equilibrium can be assumed. Due to their conceptual simplicity both the QSSA and the PEA method are still used nowadays although more sophisticated model reduction methods have been developed. Examples of use for the QSSA method and the PEA method can be found in [32, 41].

Another model reduction technique called *Invariant Constrained equilibrium Edge PreImage Curve (ICE-PIC)* has been introduced by Ren et al. in 2006 [34]. This method is based on an ICE manifold which is the union of all reaction trajectories emanating from points lying in the edge of a constrained equilibrium manifold (for more details see [34]). As the ICE manifold is constructed from reaction trajectories it is invariant. Based on this invariant constrained equilibrium edge manifold a species reconstruction can be done locally which means without having to generate the whole manifold in advance.

In [15, 44] an iterative model reduction method is presented called *Zero Derivative Principle (ZDP)*. In analogy to the model reduction method presented in this work the ZDP makes use of splitting up the ODE system $\dot{c} = f(c),\ c(t) \in \mathbb{R}^n$ into

$$\begin{aligned}\dot{c}_{\mathrm{rpv}} &= f_a(c_{\mathrm{rpv}}, c_{\mathrm{free}}), \quad c_{\mathrm{rpv}}(t) \in \mathbb{R}^{n_{\mathrm{s}}} \\ \dot{c}_{\mathrm{free}} &= f_b(c_{\mathrm{rpv}}, c_{\mathrm{free}}), \quad c_{\mathrm{free}}(t) \in \mathbb{R}^{n_{\mathrm{f}}}\end{aligned}$$

in a way that the variables c_{rpv} parameterize the slow manifold. Furthermore, it holds that $n_{\mathrm{f}} + n_{\mathrm{s}} = n$. The initial conditions $c_{\mathrm{rpv}}(0) = c_{\mathrm{rpv}}^0$ are only specified for the reaction progress variables c_{rpv}. Thus, the slow manifold is assumed to be locally given by the graph of a function $c_{\mathrm{free}} = c_{\mathrm{free}}(c_{\mathrm{rpv}})$ for which an appropriate solution $c_{\mathrm{free}}^m(c_{\mathrm{rpv}})$ is given by the $(m+1)-st$ *derivative principle*

$$\frac{\mathrm{d}^{m+1} c_{\mathrm{free}}}{\mathrm{d}t^{m+1}} = 0. \tag{1.1}$$

In contrast to the method presented in this work (where non-local information is used), (1.1) is a local condition (i.e. condition (1.1) is applied at a single point of time). Roughly spoken, differentiation 'amplifies' rapidly varying components more than slowly varying components and this is why this method can be used to identify points near the slow manifold (condition (1.1) seeks a region where the fast components are small). The motivation why the application of this condition leads to an $m-$th order approximation to the slow manifold can be found in *singular perturbation expansion theory*. Therefore it is assumed that the ODE system can be expressed in some other variables so that it can be written in a singular perturbation form

$$\begin{aligned} \varepsilon \dot{c}_{\mathrm{f}} &= f_1\left(c_{\mathrm{f}}, c_{\mathrm{s}}; \varepsilon\right), \quad c_{\mathrm{f}}(t) \in \mathbb{R}^{n_{\mathrm{f}}} \\ \dot{c}_{\mathrm{s}} &= f_2\left(c_{\mathrm{f}}, c_{\mathrm{s}}; \varepsilon\right), \quad c_{\mathrm{s}}(t) \in \mathbb{R}^{n_{\mathrm{s}}}. \end{aligned}$$

With this formulation the derivative principle (1.1) reads as

$$\frac{\mathrm{d}^{m+1} c_{\mathrm{f}}}{\mathrm{d}t^{m+1}}\left(c_{\mathrm{f}}, c_{\mathrm{s}}^0\right) = 0.$$

Since this condition consists of n_{f} nonlinear algebraic equations, the solution $c_{\mathrm{f}}^m\left(c_{\mathrm{s}}^0\right)$ cannot be computed explicitly. Thus, a numerical approximation $c_{\mathrm{f}}^{m,\#}$ of $c_{\mathrm{f}}^m\left(c_{\mathrm{s}}^0\right)$ has to be used. This $c_{\mathrm{f}}^{m,\#}$ is the last member of the sequence

$$\left\{ c_{\mathrm{f}}^{(r+1)} \equiv F_m\left(c_{\mathrm{f}}^{(r)}\right) \mid r = 1, 2, \ldots \right\}$$

with

$$F_m : \mathbb{R}^{n_{\mathrm{f}}} \to \mathbb{R}^{n_{\mathrm{f}}}, \quad F_m(c_{\mathrm{f}}) = c_{\mathrm{f}} - (-H)^{m+1}\left(\frac{\mathrm{d}^{m+1} c_{\mathrm{f}}}{\mathrm{d}t^{m+1}}\right)\left(c_{\mathrm{f}}, c_{\mathrm{s}}^0\right)$$

being the $m-$th iterative algorithm (H is an arbitrary positive number). The iteration procedure termines when $\|c_{\mathrm{f}}^{(r+1)} - c_{\mathrm{f}}^{(r)}\| < \mathrm{TOL}_m$ for a tolerance TOL_m and $r \geqslant 1$. In [44] it is proved that the $m-$th iterative algorithm containing an analytical formula for the $(m+1)-$st derivative has a fixed point $c_{\mathrm{f}} = h_m\left(c_{\mathrm{s}}^0\right)$ which coincides with the point $h\left(c_{\mathrm{s}}^0\right)$ on the slow manifold in the slow manifold expansion in ε up to order $\mathcal{O}\left(\varepsilon^{m+1}\right)$ for each $m = 0, 1, \ldots$.

Adrover et al. [1, 2] presented a method for model reduction which comes close to the approach presented in this work. Again this method is a local method. The technique is based on a geometric characterization of local tangent and normal dynamics. This description finds its justification in the theory of normal hyperbolicity: Roughly spoken, a normally hyperbolic manifold indicates that the flow along the manifold is slower than the attraction/repulsion to/from it. The method uses a ratio $r > 1$ of the local stretching (contraction) rates of vectors orthogonal to the SIM compared to those tangent to the SIM. Then this ratio is maximized. As an example a two-dimensional dynamical system is considered:

$$\dot{c} = f(c) = \begin{pmatrix} f_1(c) \\ f_2(c) \end{pmatrix}, \quad c \in \mathbb{R}^2$$

possessing a one-dimensional SIM $\mathcal{W}$. Then the stretching ratio r is given by

$$r(c) := \frac{\omega_\nu(c)}{\omega_\tau(c)} := \frac{\langle J_f(c) \cdot \hat{n}, \hat{n} \rangle}{\langle J_f(c) \cdot \hat{f}, \hat{f} \rangle}, \quad c \in \mathcal{W}$$

with $\hat{f} := \frac{f}{\|f\|}$, $\hat{n} := \frac{n}{\|n\|}$, $n := (f_2, -f_1)^T$, $\langle \cdot, \cdot \rangle$ being the scalar product, $\|\cdot\|$ indicating the norm, and $J_f(c)$ being the Jacobian matrix of $f(c)$. Here, ω_τ denotes the tangential stretching rate and ω_ν the normal stretching rate. The reduction method can be viewed as a local embedding technique: Locally projecting the dynamics onto the most slow directions. In the $n-$dimensional case ($n > 2$) the tangential stretching rate is still given by

$$\omega_\tau(c) = \langle J_f(c) \cdot \hat{f}, \hat{f} \rangle$$

while the definition of normal stretching rates is

$$\omega_\nu(c) = \max_{\hat{n} \in N\mathcal{W}_c, \|\hat{n}\|=1} \langle J_f(c) \cdot \hat{n}, \hat{n} \rangle$$

where the maximum is taken over all vectors $\hat{n}$ belonging to the normal space $N\mathcal{W}_c$ at c. This value can be computed by the largest eigenvalue of a symmetric matrix.

1.3 Outline

The structure of this thesis is as follows: In Chapter 2 an overview of the theoretical basic knowledge is presented which is necessary for understanding and discussing this work. As mentioned before model reduction is based on the multiple time scales present in the system. The analysis of ODE systems, that can be split up into fast and slow variables (splitting up of the different time scales), is performed by means of the theory of *singular perturbed systems*. Additionally, a few aspects of the theory of generic *dynamical systems* are stated. Subsequent subsection deals with *chemical reaction kinetics*. Here it is explained how to transform the chemical reaction mechanism into an ODE system. The approach for model reduction in chemical kinetics analyzed in this work is the formulation of an *optimization* problem which has to be solved. Therefore important results from the theory of optimization are presented as a last part of the theoretical aspects.

In addition, in Section 2.2 the numerical background is described. First, an *interior point method* is presented used in the optimization software package IPOPT and afterwards a *collocation method* is shown which is used for discretization of the ODE system. Additionally, it is presented how to solve the discretized dynamical system numerically. The collocation method together with the software package IPOPT are basic parts of a code – developed by Jochen Siehr – which has been adapted to the mechanisms for solving the optimization problem used for approximating SIMs in this thesis.

In Chapter 3 an historical overview of the *trajectory-based optimization approach* for model reduction in chemical kinetics is shown starting with the idea from Lebiedz in 2004 containing the computation of *Minimal Entropy Production Trajectories (MEPT)*. Over the years this optimization approach has been further developed by Lebiedz, Reinhardt, Siehr, and Winckler and therefore different versions of the optimization approach have arisen. Some important features are presented in this chapter. Additionally, the numerical solutions are presented (computed by the author) in a way that the accuracy of the solutions can be compared.

Chapter 4 presents the results. First a new formulation of the optimization problem (called *reverse mode*) is presented based on ideas of Dirk Lebiedz followed by the results achieved with this formulation. As a central part of this thesis it is analytically shown for a two-dimensional linear and a two-dimensional non-linear test mechanism that the *reverse mode* formulation characterizes the SIM exactly for an infinite time horizon in the optimization problem. Also numerical results are presented concerning these two test mechanisms and two non-linear mecha-

nisms from chemical kinetics including six species. Considering these numerical solutions, the *reverse mode* formulation seems to be a very good approach for the characterization of SIMs.

The thesis is summarized in Chapter 5 and an outlook is given. In the latter the focus is on the application to large-scale mechanisms and on the extension of analytical results.

Chapter 2

Theoretical Background

2.1 Theoretical Aspects

2.1.1 Dynamical Systems Theory for Singular Perturbation Problems

Chemical mechanisms can be described by systems of ODEs. In this work equations of the following form are considered:

$$\dot{c}(t) = \frac{\mathrm{d}c(t)}{\mathrm{d}t} = f\left(c(t)\right) \tag{2.1}$$

with $c(t) \in \mathbb{R}^n$ and $t \in \mathbb{R}$. Equations of the form (2.1) are called *vector field*, *ODE*, or *dynamical system*. A solution of (2.1) is a map $c : I \subset \mathbb{R} \to \mathbb{R}^n$, $t \mapsto c(t)$ such that $c(t)$ satisfies (2.1). ODE (2.1) is also called *vector field* because the solution $c(t)$ can be interpreted as a curve in $\mathbb{R}^n$ and (2.1) gives the tangent vector at each point of the curve. Note that the vector fields regarded in this work are *autonomous vector fields* which means the right-hand side f does not explicitly depend on time t.

Furthermore, the problems considered in this work involve two different time scales. Thus, it is assumed that there exists a diffeomorphism so that the problem (2.1) can be rewritten as the following *fast system*

$$\dot{c}_\mathrm{f} = \quad f_1\left(c_\mathrm{f}, c_\mathrm{s}; \varepsilon\right), \quad c_\mathrm{f}(t) \in \mathbb{R}^{n_\mathrm{f}} \tag{2.2a}$$

$$\dot{c}_\mathrm{s} = \varepsilon f_2\left(c_\mathrm{f}, c_\mathrm{s}; \varepsilon\right), \quad c_\mathrm{s}(t) \in \mathbb{R}^{n_\mathrm{s}} \tag{2.2b}$$

where the parameter $\varepsilon \in \mathbb{R}$ $(0 < \varepsilon \ll 1)$ measures the separation of time scales, c_f denotes the *fast variables* (c_f generally evolves at an $\mathcal{O}(1)$ rate given by the function f_1), and c_s the *slow variables* (c_s evolves at an $\mathcal{O}(\varepsilon)$ rate). Additionally it holds that $n_\mathrm{f} + n_\mathrm{s} = n$ and the functions f_1 and f_2 are C^∞ functions of c_f,

c_s, and ε in $V \times J$ with V being an open subset of $\mathbb{R}^{n_\mathrm{f}} \times \mathbb{R}^{n_\mathrm{s}}$ and J being an open interval containing $\varepsilon = 0$. In other words it is assumed that there exists an invertible change of coordinates which transforms the system (2.1) into the so-called singular perturbation form (2.2).

By introducing the *slow time* $\tau := \varepsilon t$, the system (2.2) can be reformulated as the following *slow system*:

$$\varepsilon c_\mathrm{f}' = f_1\left(c_\mathrm{f}, c_\mathrm{s}; \varepsilon\right), \quad c_\mathrm{f}(\tau) \in \mathbb{R}^{n_\mathrm{f}} \tag{2.3a}$$

$$c_\mathrm{s}' = f_2\left(c_\mathrm{f}, c_\mathrm{s}; \varepsilon\right), \quad c_\mathrm{s}(\tau) \in \mathbb{R}^{n_\mathrm{s}} \tag{2.3b}$$

where the prime $'$ denotes differentiation w.r.t. the new time τ ($' = \frac{\mathrm{d}}{\mathrm{d}\tau}$). Systems (2.1), (2.2), and (2.3) are equivalent for $\varepsilon \neq 0$ and the latter two are labeled *singular perturbation problems* based on the discontinuous limiting behavior as $\varepsilon \to 0$. For the short-term dynamics of system (2.1) the fast system (2.2) is more appropriate and for the long-term dynamics the slow system (2.3) is more applicable.

By setting $\varepsilon = 0$ the fast system (2.2) reduces to an n_f-dimensional system with c_s being a vector consisting of constant parameters:

$$\dot{c}_\mathrm{f} = f_1\left(c_\mathrm{f}, c_\mathrm{s}; 0\right) \tag{2.4a}$$

$$\dot{c}_\mathrm{s} = 0. \tag{2.4b}$$

The system (2.4) is denoted as *reduced fast system.*

In contrast to this the *reduced slow system* (slow system (2.3) with $\varepsilon = 0$) is differential-algebraic where the dimension of the ODE system decreases from $n_\mathrm{f} + n_\mathrm{s}$ to n_s:

$$0 = f_1\left(c_\mathrm{f}, c_\mathrm{s}; 0\right) \tag{2.5a}$$

$$c_\mathrm{s}' = f_2\left(c_\mathrm{f}, c_\mathrm{s}; 0\right). \tag{2.5b}$$

One of the questions one tries to answer in singular perturbation theory is the following: What is the relation between solutions of the singular perturbation problems and those of the reduced systems?

The two unperturbed systems (2.4) and (2.5) offer different insights into the limiting behavior of orbits (see Definition 2.1.3). Also geometric structures in the fast and slow regimes can be analyzed by regarding the two reduced systems.

Concepts for Systems of Ordinary Differential Equations

The following definitions and theorems establish the basic terminology from dynamical systems theory. Again the general formulation of an ODE system (2.1) is considered: $\dot{c}(t) = f\left(c(t)\right),\ c(t) \in \mathbb{R}^n$.

To distinguish a solution trajectory, an *initial condition* is specified (i.e. $c(t_0) =: c_0$).

Definition 2.1.1 (Initial Value Problem (IVP))
The ODE system (2.1) together with a specified initial condition

$$\begin{aligned} \dot{c}(t) &= f\left(c(t)\right), \quad t \in I \\ c(t_0) &= c_0 \end{aligned} \tag{2.6}$$

is called Initial Value Problem (IVP).

For a solution to an IVP being unique, certain regularity conditions have to be imposed on the right hand side f. A vector valued function $f(c)$ is said to satisfy a *Lipschitz-condition* in the interval $[t_0, t_\mathrm{f}]$ with respect to c (with the *Lipschitz-constant* $L \geqslant 0$), if for $c_1, c_2 \in \mathbb{R}^n$ it holds that

$$\|f(c_1(t)) - f(c_2(t))\| \leqslant L\|c_1(t) - c_2(t)\|$$

for all $t \in [t_0, t_\mathrm{f}]$. The function is said to satisfy a *local Lipschitz condition* if for every $c \in \mathbb{R}^n$ there exists a neighborhood $\mathcal{U}(c)$ such that f restricted to $\mathcal{U}$ satisfies a Lipschitz condition (the Lipschitz constant L can take different values on different neighborhoods). The following theorem is formulated for a non-autonomous ODE system $\dot{c}(t) = f\left(t, c(t)\right)$.

Theorem 2.1.2 (Existence and Uniqueness Theorem)
Let f be continuous on the strip $S := \{(t, c) \mid t_0 \leqslant t \leqslant t_\mathrm{f},\ c \in \mathbb{R}^n\}$ with finite t_0 and t_f and satisfy a local Lipschitz condition with respect to c. Then for every pair (t, c_0) with $t \in [t_0, t_\mathrm{f}]$ and $c_0 \in \mathbb{R}^n$ there exists exactly one function $c(t)$ with

$$\dot{c}(t) = f(t, c(t)) \quad \textit{for} \quad t \in [t_0, t_\mathrm{f}] \quad \textit{and} \quad c(t_0) = c_0.$$

Proof. See e.g. Walter [40]. □

The function f satisfies a local Lipschitz condition with respect to c if f is continuously differentiable. This means if f is continuously differentiable w.r.t. c – which is true for the ODE systems considered in this work – then a solution of the IVP (2.6) exists and is unique.

A solution $c(t)$ of (2.1) with the initial condition $c(t_0) = c_0$ (cf. IVP (2.6)) is called *trajectory* through the point c_0 at $t = t_0$. This solution is also denoted by $c(t, c_0)$.

Definition 2.1.3 (Orbit)
For a point c_0 in the phase space of (2.1) the orbit $O(c_0)$ through c_0 *is defined as the set of points in phase space which lie on a trajectory passing through c_0. For $c_0 \in \mathcal{U} \subset \mathbb{R}^n$ the orbit through c_0 is given by*

$$O(c_0) = \left\{ c \in \mathbb{R}^n \mid c = c(t, c_0), t \in I \right\}.$$

To analyze a solution of (2.1) two definitions of *stability* are stated. A solution $\bar{c}(t)$ of (2.1) is called *stable* (*Lyapunov stable*) if for any given $\varepsilon > 0$ there exists a $\delta = \delta(\varepsilon) > 0$ such that $\|\bar{c}(t) - \breve{c}(t)\| < \varepsilon$ for any solution $\breve{c}(t)$ of (2.1) that satisfies $\|\bar{c}(t^*) - \breve{c}(t^*)\| < \delta$ with $t > t^*$, $t^* \in \mathbb{R}$. Lyapunov stability means that solutions starting close to $\bar{c}(t)$ will remain close to $\bar{c}(t)$. A solution $\bar{c}(t)$ of (2.1) is called *asymptotically stable* if it is Lyapunov stable and if there exists a constant $b > 0$ such that $\lim_{t\to\infty} \|\bar{c}(t) - \breve{c}(t)\| = 0$ follows from $\|\bar{c}(t^*) - \breve{c}(t^*)\| < b$ for any solution $\breve{c}(t)$ of (2.1). In other words $\bar{c}(t)$ is asymptotically stable if nearby orbits converge to $\bar{c}(t)$ for $t \to \infty$.

An important point for studying the system dynamics are sets of points involving special properties, e.g. *fixed points*. A *fixed point* of (2.1) is a point $c^{\mathrm{eq}} \in \mathbb{R}^n$ where the function f vanishes ($f(c^{\mathrm{eq}}) = 0$). Other terms often used for *fixed point* are *equilibrium point*, *equilibrium solution*, *stationary point*, or *critical point*. In chemical kinetics they correspond to equilibrium states of the system that is being modeled.

Other more general sets of points are *invariant sets*. A set $S \subset \mathbb{R}^n$ is said to be *invariant under* $\dot{c} = f(c)$ if for any $c_0 \in S$ it holds that $c(t, c_0) \in S$ for all $t \in \mathbb{R}$. If especially $t \geqslant 0$ S is called a *positively invariant set*. An example for such invariant sets are fixed points.

In this work the focus is on invariant sets that have a special property, namely they will be *manifolds*. A *smooth manifold of dimension q* is a set of points in $\mathbb{R}^p$ ($q \leqslant p$) if each point in the set has a neighborhood that is locally C^∞ diffeomorphic to an open subset of $\mathbb{R}^q$. Thus, an invariant set S is said to be a C^k ($k \geqslant 1$) *invariant manifold* if S has the structure of a C^k differentiable manifold. Furthermore, if S is especially a positively invariant set then S is said to be a C^k *positively invariant manifold*.

Consider a closed and invariant set $\mathcal{A}$. If there exists an open neighborhood $\mathcal{U}$ of $\mathcal{A}$ such that all solutions $c(t)$ with initial solution in $\mathcal{U}$ will eventually enter $\mathcal{A}$ ($\lim_{t\to\infty} d\left(c(t), \mathcal{A}\right) = 0$ for a given metric d) then $\mathcal{A}$ is called an *attracting set*. An attracting set which contains a dense orbit is called an *attractor* of $\dot{c} = f(c)$, $c(t) \in \mathbb{R}^n$. An example for an attractor is an asymptotically stable fixed point.

Now the nature of solutions near a special solution $\bar{c}(t)$ is analyzed ($\bar{c}(t)$ denotes a solution of (2.1)). Therefore

$$c(t) = \bar{c}(t) + y$$

is regarded. After substituting into (2.1) and Taylor expansion about $\bar{c}(t)$ the following expression is achieved:

$$\dot{c} = \dot{\bar{c}}(t) + \dot{y} = f\left(\bar{c}(t)\right) + Df\left(\bar{c}(t)\right) y + \mathcal{O}\left(\|y\|^2\right)$$

with Df being the derivative of f.
Using $\dot{\bar{c}}(t) = f\left(\bar{c}(t)\right)$ leads to

$$\dot{y} = Df\left(\bar{c}(t)\right) y + \mathcal{O}\left(\|y\|^2\right).$$

The linear system

$$\dot{y} = Df\left(\bar{c}(t)\right) y \tag{2.7}$$

is considered. If $\bar{c}(t)$ is an equilibrium solution (i.e. $\bar{c}(t) = c^{\mathrm{eq}}$) then $Df\left(c^{\mathrm{eq}}\right)$ is a matrix with constant entries and by using the matrix exponential function the solution of (2.7) through the point $y(0) = y_0 \in \mathbb{R}^n$ is given by

$$y(t) = \mathrm{e}^{Df(c^{\mathrm{eq}})t} y_0. \tag{2.8}$$

The eigenvalues of $Df\left(c^{\mathrm{eq}}\right)$ determine the stability properties of c^{eq}: The equilibrium solution $c(t) = c^{\mathrm{eq}}$ of the non-linear vector field (2.1) is asymptotically stable if all eigenvalues of $Df\left(c^{\mathrm{eq}}\right)$ have negative real parts.

Definition 2.1.4 (Hyperbolic Fixed Point)
Assume c^{eq} being a fixed point of (2.1). If none of the eigenvalues of $Df\left(c^{\mathrm{eq}}\right)$ have zero real parts then c^{eq} is called a hyperbolic fixed point.

Let $c^{\mathrm{eq}} \in \mathbb{R}^n$ be an equilibrium solution of the vector field $\dot{c} = f(c)$. The associated linearized system (2.8) can be written as

$$\dot{y} = Ay, \quad y(t) \in \mathbb{R}^n \tag{2.9}$$

with $A = Df(c^{\mathrm{eq}})$ being a constant $n \times n$ matrix (Df denotes the Jacobian of f). The solution of Equation (2.9) through the point $y_0 \in \mathbb{R}^n$ is given by

$$y(t) = \mathrm{e}^{At} y_0.$$

The matrix A allows the definition of three subspaces which are all invariant subspaces of the linearized Equation (2.9):

- The stable subspace E^{s} which is spanned by the generalized eigenvectors of A corresponding to the eigenvalues of A having negative real part
  $(E^{\mathrm{s}} = \mathrm{span}\{e_1, \ldots, e_s\})$.
- The unstable subspace E^{u} which is spanned by the generalized eigenvectors of A corresponding to the eigenvalues of A having positive real part
  $(E^{\mathrm{u}} = \mathrm{span}\{e_{s+1}, \ldots, e_{s+u}\})$.
- The center subspace E^{c} which is spanned by the generalized eigenvectors of A corresponding to the eigenvalues of A having zero real part
  $(E^{\mathrm{c}} = \mathrm{span}\{e_{s+u+1}, \ldots, e_{s+u+c}\})$.

It holds that $s+u+c = n$. The Euclidean space $\mathbb{R}^n$ can be represented as direct sum of these three subspaces. The non-linear system $\dot{c} = f(c)$ (corresponding to the associated linearized one (2.9)) has invariant manifolds: The stable manifold is tangent to the stable subspace E^{s} at c^{eq} and has the same dimension and the unstable manifold is tangent to the unstable subspace E^{u} at c^{eq} and has the same dimension. The *center manifold* is tangent to the center subspace E^{c} at c^{eq}. Thus, the center manifold of an equilibrium solution of a vector field consists of orbits whose behavior is not controlled by either the attraction of the stable manifold or the repulsion of the unstable manifold.

Theorem 2.1.5 (Center Manifold Theorem)
Let f be a C^r vector field on $\mathbb{R}^n$ vanishing at c^{eq} ($f(c^{\mathrm{eq}}) = 0$) and let $A = Df(c^{\mathrm{eq}})$ be the Jacobian of f evaluated at c^{eq}. Divide the spectrum of A into three subsets σ_s, σ_c, and σ_u with

$$\mathrm{Re}(\lambda) \begin{cases} < 0 & \text{if } \lambda \in \sigma_s \\ = 0 & \text{if } \lambda \in \sigma_c \\ > 0 & \text{if } \lambda \in \sigma_u. \end{cases}$$

The (generalized) eigenspaces of σ_s, σ_c, and σ_u are E^{s}, E^{c}, and E^{u} respectively. Then there exist C^r stable and unstable invariant manifolds W^{u} and W^{s} tangent to E^{u} and E^{s} at c^{eq} and a C^{r-1} center manifold W^{c} tangent to E^{c} at c^{eq}. The manifolds W^{u}, W^{s}, and W^{c} are all invariant for the flow of f. The stable and unstable manifolds are unique but W^{c} need not be.

Proof. See e.g. Guckenheimer, Holmes [18]. □

If the eigenvalues of the center subspace are all precisely zero – rather than just real part zero – then a center manifold is called a *slow manifold*.

The dynamical systems used in this work have a special property, namely they are all *dissipative*. Dissipative systems are systems that are not *conservative*. Conservative systems are defined by the following theorem:

Theorem 2.1.6 (Liouville)
Consider again the general autonomous vector field $\dot{c} = f(c)$, $c(t) \in \mathbb{R}^n$. *Suppose that the vector field is* divergence free, *i.e.* $\nabla \cdot f = 0$. *Then for any domain* $D_0 \subset \mathbb{R}^n$ *it holds that*

$$V(t) = V(0)$$

with $V(0)$ *being the volume of* D_0 *and* $V(t)$ *being the volume of* $\phi_t(D_0)$ *(*$\phi_t(D_0)$ *is the evolution of* D_0 *under the flow* $\phi_t(\cdot)$*, that is generated by the vector field).*

Proof. See e.g. Wiggins [42]. □

Concepts for Singular Perturbation Problems

To recapitulate, the Geometric Singular Perturbation Theory (GSPT) deals with problems with clear separation of time-scales t and $\tau = \varepsilon t$, with $0 < \varepsilon \ll 1$ being a small parameter. Furthermore, it constructs invariant manifolds to study solutions of singularly perturbed dynamical systems.

Again the singular perturbation problems (2.2), (2.3) and the corresponding reduced systems (2.4), (2.5) are considered. Regarding system (2.5), the set of points $(c_\mathrm{f}, c_\mathrm{s}) \in V \subset \mathbb{R}^{n_\mathrm{f}} \times \mathbb{R}^{n_\mathrm{s}}$ for which $f_1(c_\mathrm{f}, c_\mathrm{s}; 0) = 0$ is called the *slow manifold* $\mathcal{W}_0$. If it is assumed that the eigenvalues of $D_{c_\mathrm{f}} f_1$ (Jacobian of f_1 w.r.t. c_f) have all negative real part, then the implicit function theorem guarantees the existence of a smooth function $z_0 : K \to \mathbb{R}^{n_\mathrm{f}}$ (K being a compact domain $K \subset \mathbb{R}^{n_\mathrm{s}}$), which represents this slow manifold by the equation

$$c_\mathrm{f} = z_0(c_\mathrm{s}).$$

Then the dynamics of (2.5) on the slow manifold $\mathcal{W}_0$ is governed by the equation

$$c_\mathrm{s}' = f_2\left(z_0(c_\mathrm{s}), c_\mathrm{s}; 0\right).$$

Regarding system (2.2) with $\varepsilon = 0$, $\mathcal{W}_0$ is a manifold of equilibrium points, since by definition $\dot{c}_\mathrm{f} = 0$ at all points $\left(z_0(c_\mathrm{s}), c_\mathrm{s}; 0\right)$ at which f_1 vanishes. This implicates $\mathcal{W}_0$ being invariant.

The fact that the slow manifold $\mathcal{W}_0$ consists of equilibrium points in the reduced fast system (2.4) contrasts highly with the result that there is dynamics on $\mathcal{W}_0$ when $\mathcal{W}_0$ is analyzed in the reduced slow system (2.5), but both perspectives are useful. In the following, this work will focus exclusively on those manifolds in which, when $\varepsilon = 0$, each point $\left(z_0(c_\mathrm{s}), c_\mathrm{s}\right)$ on $\mathcal{W}_0$ is a hyperbolic fixed point of the reduced fast system (2.4). In these systems the invariant manifold $\mathcal{W}_0$ is said to be *normally hyperbolic*.

Example: Linear Planar System

As an example the following linear two-dimensional decoupled ODE system is considered:

$$\dot{c}_\mathrm{f} = -\ c_\mathrm{f} \tag{2.10a}$$
$$\dot{c}_\mathrm{s} = -\varepsilon c_\mathrm{s} \tag{2.10b}$$

with $0 < \varepsilon \ll 1$. This is an example for the fast system (2.2) with $n_\mathrm{f}, n_\mathrm{s} = 1$. The Jacobian of this system is the 2×2 diagonal matrix with eigenvalues -1 and $-\varepsilon$. This implicates the origin being a hyperbolic fixed point for all $\varepsilon \neq 0$. Moreover, the origin is the only fixed point when $\varepsilon \neq 0$. System (2.10) is an example for a situation, where the hyperbolicity of this fixed point is lost when $\varepsilon = 0$.

Using $\big(c_\mathrm{f}(0), c_\mathrm{s}(0); \varepsilon\big)$ as initial data, the general solution is given by

$$c_\mathrm{f}(t) = c_\mathrm{f}(0)\mathrm{e}^{-t}$$
$$c_\mathrm{s}(t) = c_\mathrm{s}(0)\mathrm{e}^{-\varepsilon t}.$$

First the geometric structure of the system (2.10) is discussed for $\varepsilon = 0$. Afterwards the full system is considered.

The reduced fast system (cf. (2.4)) is

$$\dot{c}_\mathrm{f} = -c_\mathrm{f}$$
$$\dot{c}_\mathrm{s} = \quad 0.$$

Regarding this reduced model in the phase space of system (2.10), it can be seen that the c_s–axis is a line of fixed points, and hence an invariant manifold. The fast component of the vector field, $f_1(c_\mathrm{f}, c_\mathrm{s}; 0) = -c_\mathrm{f}$, linearized at the fixed point $c_\mathrm{f} = 0$ has -1 as eigenvalue for each c_s, what implicates the c_s–axis being a normally hyperbolic invariant manifold (denoted as $\mathcal{W}_0$).

The *fast fibers* $F^0_{c_s}$ are the lines of constant c_s for each c_s and at the same time these lines are invariant sets. The points $(0, c_\mathrm{s})$ at which these fast fibers are attached to the manifold $\mathcal{W}_0$ are called the *basepoints* of the fibers.

By analyzing the case when $0 < \varepsilon \ll 1$, the c_s–axis is again an invariant manifold labeled as $\mathcal{W}_\varepsilon$. The flow on this manifold is slow, governed by the slow component of the system:

$$\varepsilon c_\mathrm{f}' = -c_\mathrm{f} \tag{2.11a}$$
$$c_\mathrm{s}' = -c_\mathrm{s}. \tag{2.11b}$$

The individual fibers (lines c_s =constant) are labeled by $F^\varepsilon_{c_\mathrm{s}}$, where c_s denotes the c_s–coordinate of the fiber's basepoint. These fibers are not invariant individually relative to (2.11) (in contrast to the case $\varepsilon = 0$). A trajectory that starts out at the initial condition $\big(c_\mathrm{f}(0), c_\mathrm{s}(0)\big)$ on $F^\varepsilon_{c_\mathrm{s}(0)}$ evolves in a way that $\big(c_\mathrm{f}(\tau), c_\mathrm{s}(\tau)\big)$ lies on $F^\varepsilon_{\Phi_\tau(c_\mathrm{s}(0))}$ with Φ being the flow of the full system. The evolution of an arbitrary initial condition $\big(c_\mathrm{f}(0), c_\mathrm{s}(0)\big) \neq (0,0)$ can be decomposed into

- a slow component given by the slow motion of the fibers' basepoints along the manifold $\mathcal{W}_\varepsilon$.
- a fast component in the normal direction governed by the exponential rate of contraction along the fast fibers.

The Method of Matched Asymptotic Expansions and its Relation to the Geometric Approach for Example (2.10)

The method of matched asymptotic expansions tries to write the solution of (2.10) through a fixed initial condition $\big(c_\mathrm{f}(0), c_\mathrm{s}(0)\big)$ (positive and independent of ε) as a power series in ε:

$$\begin{aligned} c_\mathrm{f}^\mathrm{inner}(t,\varepsilon) &= c_{\mathrm{f},0}(t) + \varepsilon c_{\mathrm{f},1}(t) + \varepsilon^2 c_{\mathrm{f},2}(t) + \mathcal{O}(\varepsilon^3) \\ c_\mathrm{s}^\mathrm{inner}(t,\varepsilon) &= c_{\mathrm{s},0}(t) + \varepsilon c_{\mathrm{s},1}(t) + \varepsilon^2 c_{\mathrm{s},2}(t) + \mathcal{O}(\varepsilon^3). \end{aligned}$$

Subsituting these expansions into (2.10) yields:

$$\begin{aligned} c_\mathrm{f}^\mathrm{inner}(t,\varepsilon) &= c_\mathrm{f}(0)\mathrm{e}^{-t} \\ c_\mathrm{s}^\mathrm{inner}(t,\varepsilon) &= c_\mathrm{s}(0)\left(1 - \varepsilon t + \varepsilon^2 \frac{t^2}{2} + \mathcal{O}(\varepsilon^3)\right). \end{aligned}$$

This expansion is called *inner expansion* and the corresponding system (2.10) is called the *inner equation*.

Regarding system (2.11), the power series expansion of the solution can be written as (coefficients are functions of τ):

$$\begin{aligned} c_\mathrm{f}^\mathrm{outer}(\tau,\varepsilon) &= c_{\mathrm{f},0}(\tau) + \varepsilon c_{\mathrm{f},1}(\tau) + \varepsilon^2 c_{\mathrm{f},2}(\tau) + \mathcal{O}(\varepsilon^3) \\ c_\mathrm{s}^\mathrm{outer}(\tau,\varepsilon) &= c_{\mathrm{s},0}(\tau) + \text{h.o.t.} \end{aligned}$$

where h.o.t. denotes higher order terms. The same procedure as above (substituting these expansions into system (2.11)) yields:

$$\begin{aligned} c_\mathrm{f}^\mathrm{outer}(\tau,\varepsilon) &= 0 + \varepsilon \cdot 0 + \varepsilon^2 \cdot 0 + \cdots + c_\mathrm{f}(0)\mathrm{e}^{-\tau} \\ c_\mathrm{s}^\mathrm{outer}(\tau,\varepsilon) &= c_\mathrm{s}(0)\mathrm{e}^{-\tau}. \end{aligned}$$

According to the inner expansions, these equations are labeled *outer expansions* and the corresponding system (2.11) is called the *outer equation.*

There is a relation between the geometric aspects and the method of matched asymptotic expansions. The leading order term in the inner expansion ($c_\mathrm{f}(t) = c_\mathrm{f}(0)\mathrm{e}^{-t}, c_\mathrm{s}(t) = c_\mathrm{s}(0)$) is the solution along the unperturbed fiber $F^0_{c_\mathrm{s}(0)}$, whereas the leading order term in the outer expansion ($c_\mathrm{f}(\tau) = 0, c_\mathrm{s}(\tau) = c_\mathrm{s}(0)\mathrm{e}^{-\tau}$) corresponds to the evolution of that fiber's basepoint along $\mathcal{W}_0$. The extended inner expansion describes the initial evolution of points on $F^\varepsilon_{c_\mathrm{s}(0)}$ as well as the motion of points on the fibers close to $\mathcal{W}_\varepsilon$. On the other hand, the extended outer expansion describes the evolution of the basepoints on $\mathcal{W}_\varepsilon$ as well as the evolution of points close to $\mathcal{W}_\varepsilon$.

Next, a basic result from Fenichel theory [10, 11, 12, 13, 20] is stated implicating the persistence of $\mathcal{W}_0$ as slow manifold (provided that special assumtions are fulfilled), so for all $0 < \varepsilon \ll 1$ there exists a slow manifold $\mathcal{W}_\varepsilon$.

Fenichel Theory for Singular Perturbation Problems

By considering the general system (2.2), Fenichel geomertric theory [10, 11, 12, 13, 20] states a theorem for boundaryless compact manifolds. For these theorems the following additional assumptions on the system (2.2) are needed:

1. A compact manifold $\mathcal{W}_0$ with boundary (contained in $\{(c_\mathrm{f}, c_\mathrm{s}) : f_1(c_\mathrm{f}, c_\mathrm{s}; 0) = 0\}$) exists and is given by a graph of a C^∞ function $c_\mathrm{f} = z_0(c_\mathrm{s})$ for $c_\mathrm{s} \in D \subset \mathbb{R}^{n_\mathrm{s}}$ with D being a compact, simply connected domain with its boundary being a $(n-1)$ dimensional C^∞ submanifold. Furthermore, D is overflowing invariant with respect to (2.3) when $\varepsilon = 0$. (A compact manifold with boundary is said to be *overflowing invariant* when
   - the vector field is tangent to the manifold at every point inside the manifold.
   - the vector field points outward at every point on the boundary of the manifold.)
2. The set $\mathcal{W}_0$ ist normally hyperbolic relative to (2.4). Furthermore, it is required that for all points $p \in \mathcal{W}_0$ there are k (resp., l) eigenvalues of $D_{c_\mathrm{f}} f_1(p; 0)$ (derivative of f_1 w.r.t. c_f) with positive (resp., negative) real parts bounded away from zero with $k + l = n_\mathrm{f}$.

Before formulating the Fenichel Theorem it is necessary to give the definition of a *locally invariant manifold.* An open subset S is said to be *locally invariant* w.r.t. an open set T under the system $\dot{c} = f(c)$ if S is a subset of T and if any trajectory leaving S simultaneously leaves T. If the set of points defining a manifold is a

locally invariant set, then the manifold is said to be a *locally invariant manifold* of the system $\dot{c} = f(c)$.

Theorem 2.1.7
Consider system (2.2) satisfying the additional assumptions 1. *and* 2. *For a sufficiently small* $\varepsilon > 0$ *there exists a* C^r *function (with* $r < +\infty$*)* $z_\varepsilon(c_s;\varepsilon)$ *defined on* D *such that the manifold* $\mathcal{W}_\varepsilon = \{(c_f, c_s) : c_f = z_\varepsilon(c_s;\varepsilon)\}$ *is locally invariant under (2.2). Furthermore,* $\mathcal{W}_\varepsilon$ *is* C^r $\mathcal{O}(\varepsilon)$ *close to* $\mathcal{W}_0$.

For the proof of Theorem 2.1.7 see e.g. [21].

The manifold $\mathcal{W}_\varepsilon$ from Theorem 2.1.7 is called *slow manifold* for $0 < \varepsilon \ll 1$.

Note that the function $z_\varepsilon(c_\mathrm{s};\varepsilon)$ is generally nonunique. Furthermore, $z_\varepsilon(c_\mathrm{s};\varepsilon)$ admits a perturbation expansion

$$z_\varepsilon(c_\mathrm{s};\varepsilon) = z_0(c_\mathrm{s}) + \varepsilon z_1(c_\mathrm{s}) + \mathcal{O}(\varepsilon^2)$$

which is plugged into the *invariance equation*

$$\varepsilon D_{c_\mathrm{s}} z_\varepsilon(c_\mathrm{s};\varepsilon) \cdot f_2\left(z_\varepsilon(c_\mathrm{s};\varepsilon), c_\mathrm{s};\varepsilon\right) = f_1\left(z_\varepsilon(c_\mathrm{s};\varepsilon), c_\mathrm{s};\varepsilon\right)$$

to solve order by order for $z_\varepsilon(c_\mathrm{s};\varepsilon)$ (the expression $D_{c_\mathrm{s}} z_\varepsilon(c_\mathrm{s};\varepsilon)$ denotes the derivative of $z_\varepsilon(c_\mathrm{s};\varepsilon)$ w.r.t. c_s). Fenichel theory states that the system (2.2) – under special assumptions – possesses a slow manifold.

In this thesis, ODE systems of the form (2.1) are considered assuming that there exists a diffeomorphism which transforms such ODE systems into singular perturbed systems. By reason of model reduction, the aim of this work is the description of the long-term dynamics of the system and hence the computation of such slow manifolds $\mathcal{W}_\varepsilon$.

2.1.2 Chemical Reaction Kinetics

The dynamical systems considered in this work are chemical reaction mechanisms (amongst others), which can be modeled by systems of ODEs. This is why this subsection points out a fundamental knowledge of *chemical reaction kinetics*.

It is assumed that there are n chemical species – denoted as $\mathrm{A}_1, \ldots, \mathrm{A}_n$ – participating in a chemical reaction mechanism, that takes place in a *closed system* (a system, that exchanges energy, but not matter with its exterior). This reaction mechanism – composed of m reactions – is given by

$$\sum_{s=1}^{n} \nu_{rs}^{(e)} \mathrm{A}_s \underset{k_{r,-}}{\overset{k_{r,+}}{\rightleftharpoons}} \sum_{s=1}^{n} \nu_{rs}^{(p)} \mathrm{A}_s, \quad r = 1, \ldots, m$$

where each r denotes an *elementary reaction* r. Here $\nu_{rs}^{(e)}$ and $\nu_{rs}^{(p)}$ denote stoichiometric coefficients of *educts/reactants* and *products* in reaction r and $k_{r,+}$ and $k_{r,-}$ denote the *rate coefficients* of an elementary reaction r.

The concentration of a chemical species A_i is $c_i = \frac{n_i}{V}$ with n_i being the amount of substance of that species and V being the volume. By reason of V being constant in the mechanisms considered in this work, the *reaction kinetic equations* are given by

$$\dot{c} = \sum_{r=1}^{m} \nu_r W_r(c) \tag{2.12}$$

where ν_r stands for the vector $\nu_r = (\nu_{r1}^{(p)} - \nu_{r1}^{(e)}, \ldots, \nu_{rn}^{(p)} - \nu_{rn}^{(e)})^T$ and $W_r(c)$ is the *reaction rate function* of reaction r, which is defined by the *mass action law*

$$W_r(c) = W_{r,+}(c) - W_{r,-}(c) = k_{r,+} \prod_{s=1}^{n} c_s^{\nu_{rs}^{(e)}} - k_{r,-} \prod_{s=1}^{n} c_s^{\nu_{rs}^{(p)}}.$$

Thus, the rate coefficients $k_{r,+}$ and $k_{r,-}$ are the constants of the *direct* ($W_{r,+}(c)$) and of the *inverse* ($W_{r,-}(c)$) *reaction rates* of the rth elementary reaction and can be computed by the *Arrhenius law*, which is given by

$$k_{r,\pm} = A_{r,\pm} T^{b_{r,\pm}} \exp\left(-\frac{E_{a,r,\pm}}{RT}\right).$$

Here $A_{r,\pm}$ and $b_{r,\pm}$ are constants, $E_{a,r,\pm}$ is the *activation energy*, R is the *gas constant* ($R = 8.314472\ \mathrm{J/(K \cdot mol)}$), and T denotes the temperature ($T =$ const in the mechanisms considered in this thesis). Furthermore, at chemical equilibrium (denoted as c^{eq}) it holds that

$$W_{r,+}(c^{\mathrm{eq}}) = W_{r,-}(c^{\mathrm{eq}}) \quad \text{for all } r = 1, \ldots, m.$$

As mentioned above, the systems considered in this work have isochoric ($V =$ const) and isothermal ($T =$ const) conditions and in this case a *Lyapunov function* is known:

$$\mathcal{V}_{V,T} = \frac{U}{k_B T} - \frac{S}{k_B}$$

with U being the *internal energy*, S being the *entropy*, and k_B denotes the *Boltzmann constant* (see [17]). In the context of dynamical systems ($\dot{c} = f(c),\ c(t) \in \mathbb{R}^n$, e.g. (2.12)) a *Lyapunov function* is a C^1-function $\mathcal{V} : \mathcal{U} \to \mathbb{R}$ in a neighborhood $\mathcal{U}$ of a fixed point c^{eq}, if the following properties are satisfied:

1. $\mathcal{V}(c^{\mathrm{eq}}) = 0$
2. $\mathcal{V}(c) > 0$ if $c \neq c^{\mathrm{eq}}$
3. $\dfrac{\mathrm{d}\mathcal{V}(c)}{\mathrm{d}t} \leqslant 0$ in $\mathcal{U} \setminus \{c^{\mathrm{eq}}\}$.

As a Lyapunov function is known for the chemical dynamical systems used in this work, the following theorem is applicable:

Theorem 2.1.8
If a Lyapunov function $\mathcal{V}$ exists for a dynamical system $\dot{c} = f(c)$ with a fixed point c^{eq}, then c^{eq} is a stable fixed point. Moreover, if strict inequality holds for 3. *c^{eq} is asymptotically stable.*

Proof. See e.g. Wiggins [42]. □

2.1.3 Optimization

In this thesis a model reduction method is proposed which is formulated as an optimization problem where a functional has to be minimized under certain constraints comprising an ODE system. After discretization of the ODE constraint via *collocation* the resulting *Non-Linear Programming (NLP) problem* is solved by using a code developed by Jochen Siehr including the software package IPOPT by Wächter and Biegler [39]. In this software package an *interior point method* is implemented which is based on the theory of *optimization* [31] (e.g. *Karush–Kuhn–Tucker conditions*).

The general form of a finite-dimensional NLP is the following:

$$\min_{\omega \in \mathbb{R}^{n_\omega}} F(\omega) \tag{2.13a}$$

subject to

$$G(\omega) = 0 \tag{2.13b}$$
$$H(\omega) \geqslant 0 \tag{2.13c}$$

with $F : \mathbb{R}^{n_\omega} \to \mathbb{R}$, $G : \mathbb{R}^{n_\omega} \to \mathbb{R}^{n_G}$, and $H : \mathbb{R}^{n_\omega} \to \mathbb{R}^{n_H}$ being twice continuously differentiable. The function F is called *objective function* whereas the functions G and H are the *constraints*: The *equality constraints* G and the *inequality constraints* H.

Definition 2.1.9 (Feasibility and Optimality)
The point $\omega^* \in S = \{\omega \mid G(\omega) = 0,\ H(\omega) \geqslant 0\}$ *is called* feasible point *and* S *is called* feasible set*. A feasible point* ω^* *is called a* local minimizer *of NLP (2.13) if there exists a neighborhood* $\mathcal{U}_\varepsilon(\omega^*)$ *of* ω^* *such that* $F(\omega^*) \leqslant F(\omega)$ *for all* $\omega \in \mathcal{U}_\varepsilon(\omega^*) \cap S$*. The inequality constraint* $H_i(\omega) \geqslant 0$ *is called* active *if* $H_i(\omega) = 0$*. All active inequality constraints at the feasible point* ω *are denoted by* $H^{\text{act}}(\omega)$*. A feasible point* ω *is called a* regular point *if the Jacobian of the active constraints* $\nabla \tilde{G}(\omega)^T := \nabla \begin{pmatrix} G(\omega) \\ H^{\text{act}}(\omega) \end{pmatrix}^T$ *has full rank (*$\nabla_\omega G(\omega) := \left(\frac{\partial G}{\partial \omega}(\omega)\right)^T$*).*

The *Lagrangian function* $\mathcal{L}$ is defined as

$$\mathcal{L}(\omega, \lambda, \mu) := F(\omega) - \lambda^T G(\omega) - \mu^T H(\omega)$$

with $\lambda \in \mathbb{R}^{n_G}$ being the *Lagrange multiplier (vector)* of the equality constraints and $\mu \in \mathbb{R}^{n_H}$ being the *Lagrange multiplier (vector)* of the inequality constraints.

Theorem 2.1.10 (Karush–Kuhn–Tucker Necessary Conditions)
Assume ω^* being a local minimizer of (2.13) and a regular point. Then, there exist Lagrange multiplier vectors $\lambda^* \in \mathbb{R}^{n_G}$ and $\mu^* \in \mathbb{R}^{n_H}$ such that $(\omega^*, \lambda^*, \mu^*)$ satisfy the following necessary conditions:

$$\nabla_\omega \mathcal{L}\left(\omega^*, \lambda^*, \mu^*\right) = 0 \tag{2.14a}$$
$$G\left(\omega^*\right) = 0 \tag{2.14b}$$
$$H\left(\omega^*\right) \geqslant 0 \tag{2.14c}$$
$$\mu^* \geqslant 0 \tag{2.14d}$$
$$\mu_j^* H_j(\omega^*) = 0, \quad j = 1, \ldots, n_H \tag{2.14e}$$

These conditions are called Karush–Kuhn–Tucker necessary conditions *or* KKT conditions.

Proof. See e.g. Nocedal and Wright [31]. □

The *KKT conditions* play an important role for numerically solving the NLP by using an *interior point method* (see Subsection 2.2.1). For more details see [31]. A triple $(\omega^*, \lambda^*, \mu^*)$ which satisfies the necessary Karush–Kuhn–Tucker conditions (2.14) is called a *stationary point* or *Karush–Kuhn–Tucker (KKT) point.*

In this thesis the general problem can be formulated as the following optimization problem:

$$\min_{c(\cdot)} \int_{t_0}^{t_\mathrm{f}} L\left(c(t), p\right) \, \mathrm{d}t \tag{2.15a}$$

subject to

$$\dot{c}(t) - f\left(c(t), p\right) = 0, \quad \forall t \in [t_0, t_\mathrm{f}] \tag{2.15b}$$
$$r_0(c(t_0), p) + r_\mathrm{f}\left(c(t_\mathrm{f}), p\right) = 0 \tag{2.15c}$$

where t_0 and t_f denote the initial and final time, respectively, and the functions L, g, r_0, and r_f are at least twice continuously differentiable. Inequality constraints (2.13c) are not present in this formulation. A system of autonomous ODE's enters the optimization problem formulation as an equality constraint (2.15b) which describes the system dynamics of chemical kinetics (see Subsection 2.1.2). Here $c(t) \in \mathbb{R}^{n_c}$ denotes the differential state vector, $t \in \mathbb{R}$ time, and $p \in \mathbb{R}^{n_p}$ is a vector containing constant system parameters (reaction coefficients in chemical kinetics). Additionally there are boundary constraints (2.15c) which can be used e.g. to fix concentrations of chemical species at a given point of time.

2.2 Numerical Aspects

After ODE discretization via *collocation* the resulting *Non-Linear Programming problem (NLP)* which is used for the model reduction can be solved as a standard NLP via the *Interior Point (IP) method*. In general, one has to decide how to treat the differential equation constraint and the objective functional. It is often beneficial to have an 'all at once' approach that couples simulation and optimization via explicit discretization of the ODE constraint. This so-called simultaneous approach has the advantage of introducing more freedom into the optimization problem, since the differential equation model does not have to be solved exactly in each iteration of the optimization. Especially for highly unstable ODE problems a fully discrete *collocation approach* seems appropriate for the ODE constraint. On a predefined time grid the collocation method constructs polynomials obeying the differential equation at a certain number of nodes depending on its degree. For the numerical solution of the ODEs presented in this work a *Radau-method* with linear, quadratic, and cubic polynomials is used.

The NLP is solved numerically by using the robust IP method implemented in IPOPT [39] including linear algebra solvers of the HSL routines [19]. The required derivatives are computed by using the open source automatic differentiation package CppAD [4]. Plots have been generated using MATLAB®.

2.2.1 Interior Point Method

In the software package IPOPT a *primal-dual interior-point filter line-search algorithm* for large-scale programming is implemented. As this program is used for the computations done in this thesis for solving the optimization problem numerically the algorithm is motivated in this subsection.

The following problem is considered:

$$\min_{\omega \in \mathbb{R}^{n_\omega}} F(\omega) \tag{2.16a}$$

subject to

$$G(\omega) = 0 \tag{2.16b}$$

$$\omega \geqslant 0. \tag{2.16c}$$

The algorithm computes approximate solutions for a sequence of subproblems (barrier problems)

$$\min_{\omega \in \mathbb{R}^{n_\omega}} \quad \phi_\nu(\omega) := F(\omega) + \nu \sum_{i=1}^{n_\omega} \ln\left(\omega^{(i)}\right) \tag{2.17a}$$

subject to

$$G(\omega) = 0 \tag{2.17b}$$

for a decreasing sequence of barrier parameters ν converging to zero. This is equivalent to applying a homotopy method to the primal-dual equations:

$$\nabla F(\omega) + \nabla G(\omega)\lambda - \mu = 0 \tag{2.18a}$$
$$G(\omega) = 0 \tag{2.18b}$$
$$\Omega M e - \nu e = 0 \tag{2.18c}$$

($\Omega := \operatorname{diag}(\omega)$, $M := \operatorname{diag}(\mu)$, $e := (1, 1, 1, \ldots, 1)^T$).
Here ν is the homotopy parameter which converges to zero and $\lambda \in \mathbb{R}^{n_G}$ and $\mu \in \mathbb{R}^{n_\omega}$ are the Lagrange multipliers corresponding to (2.16b) and (2.16c), respectively. Equations (2.18) can also be seen as the Karush–Kuhn–Tucker conditions for the original problem (2.16) for $\nu = 0$ and $\omega, \mu \geqslant 0$. First the presented algorithm computes an approximate solution to problem (2.17) for fixed ν. Then it decreases the barrier parameter and continues solving the next barrier problem based on the previous approximate solution.

A damped Newton's method is applied to the Equations (2.18) for solving the barrier problem (2.17) for a fixed value ν_j.

$$\begin{pmatrix} W_k & A_k & -I \\ A_k^T & 0 & 0 \\ M_k & 0 & \Omega_k \end{pmatrix} \begin{pmatrix} d_k^x \omega \mathrm{d}_k^\lambda \\ d_k^\mu \end{pmatrix} = - \begin{pmatrix} \nabla F(\omega_k) + A_k \lambda_k - \mu_k \\ G(\omega_k) \\ \Omega_k M_k e - \nu_j e \end{pmatrix}$$

with $A_k := \nabla G(\omega_k)$, $(d_k^\omega, d_k^\lambda, d_k^\mu)$ being the search directions and W_k being the Hessian $\nabla^2_{\omega\omega}\mathcal{L}(\omega_k, \lambda_k, \mu_k)$ of the Lagrangian function for problem (2.16):

$$\mathcal{L}(\omega, \lambda, \mu) := F(\omega) + G(\omega)^T \lambda - \mu.$$

The proposed method computes the solution by first solving the smaller symmetric linear system

$$\begin{pmatrix} W_k + \Sigma_k & A_k \\ A_k^T & 0 \end{pmatrix} \begin{pmatrix} d_k^\omega \\ d_k^\lambda \end{pmatrix} = - \begin{pmatrix} \nabla \phi_{\nu_j}(\omega_k) + A_k \lambda_k \\ G(\omega_k) \end{pmatrix} \tag{2.19}$$

with $\Sigma_k := \Omega_k^{-1} M_k$ and subsequently computing the vector d_k^μ via

$$d_k^\mu = \nu_j \Omega_k^{-1} e - \mu_k - \Sigma_k d_k^\omega. \tag{2.20}$$

It is necessary to modify the iteration matrix of Equation (2.19) to ensure the existence of a solution to (2.19) (the iteration matrix in (2.19) is singular if A_k does not have full rank) and to guarantee certain properties for the line-search filter method (therefore the matrix in the top-left block in (2.19) – projected onto

the null space of the constraint Jacobian A_k^T – has to be positive definite). Hence the following linear system is used in the algorithm:

$$\begin{pmatrix} W_k + \Sigma_k + \delta_w I & A_k \\ A_k^T & -\delta_c I \end{pmatrix} \begin{pmatrix} d_k^\omega \\ d_k^\lambda \end{pmatrix} = - \begin{pmatrix} \nabla \phi_{\nu_j}(\omega_k) + A_k \lambda_k \\ G(\omega_k) \end{pmatrix} \tag{2.21}$$

with $\delta_w, \delta_c \geqslant 0$.

After computation of the search directions from (2.20) and (2.21) the next iteration is given by:

$$\begin{aligned} \omega_{k+1} &:= \omega_k + \alpha_k d_k^\omega \\ \lambda_{k+1} &:= \lambda_k + \alpha_k d_k^\lambda \\ \mu_{k+1} &:= \mu_k + \alpha_k^\mu d_k^\mu \end{aligned}$$

where $\alpha_k, \alpha_k^\mu \in (0, 1]$ denote the step sizes.

In order to ensure global convergence a line-search filter method by Fletcher and Leyffer [14] is used. In this process the step sizes α_k, α_k^μ are chosen in such a way that the objective function $\phi_\nu(\omega)$ or the constraint violation is minimized in the subsequent step. For more details see [38, 39].

2.2.2 Collocation Method

As the system dynamics enter the optimization problem as an ODE system constraint, this system has to be solved numerically. Therefore a *collocation method* is used in this work which is presented below.

The vector field

$$\dot{c}\,(t) = f\left(c\,(t)\right), \quad c\,(t) \in \mathbb{R}^n$$

with fixed value

$$c\,(t_*) = c^{t_*}$$

is considered. This ODE system is to be solved over the interval $[t_*, t_* + h]$. Therefore the collocation points are denoted by

$$0 \leqslant c_1 < c_2 < \cdots < c_s \leqslant 1.$$

By using the corresponding collocation method the solution c is approximated by a polynomial p of degree s which satisfies the following $s+1$ collocation conditions:

- $p(t_*) = c^{t_*}$
- $\dot{p}\,(t_* + c_i h) = f\left(p\,(t_* + c_i h)\right), \quad i = 1, \ldots, s.$

In this work s is chosen as $s = 1$, $s = 2$, or $s = 3$.

These conditions lead to the following expression (see [9] for more details):

$$p\,(t_* + h) = c^{t_*} + h \sum_{j=1}^{s} b_j k_j \tag{2.22}$$

with

$$k_i = f\left(c^{t_*} + h \sum_{j=1}^{s} a_{ij} k_j\right). \tag{2.23}$$

The choice of the values for c_i, a_{ij}, and b_j is dependent on the collocation method which is used. In this work a *Radau-method* with linear, quadratic, or cubic polynomials is used for the numerical solution of the ODE constraint and thus the values of the coefficients are listed in the Tables 2.1–2.4:

Table 2.1: General scheme of the coefficients c_i, a_{ij}, and b_j in (2.22) and (2.23) ($s = n$).

c_1	a_{11}	a_{12}	$\cdots$	a_{1n}
c_2	a_{21}	a_{22}	$\cdots$	a_{2n}
$\vdots$	$\vdots$	$\vdots$	$\ddots$	$\vdots$
c_n	a_{n1}	a_{n2}	$\cdots$	a_{nn}
	b_1	b_2	$\cdots$	b_n

Table 2.2: Values of the coefficients c_i, a_{ij}, and b_j (cf. Table 2.1). Radau-method: Linear polynomials ($s = 1$, i.e. $i = j = 1$).

1	1
	1

Table 2.3: Values of the coefficients c_i, a_{ij}, and b_j (cf. Table 2.1). Radau-method: Quadratic polynomials (s=2).

$\frac{1}{3}$	$\frac{5}{12}$	$-\frac{5}{12}$
1	$\frac{3}{4}$	$\frac{1}{4}$
	$\frac{3}{4}$	$\frac{1}{4}$

Table 2.4: Values of the coefficients c_i, a_{ij}, and b_j (cf. Table 2.1). Radau-method: Cubic polynomials (s=3).

$\frac{4-\sqrt{6}}{10}$	$\frac{88-7\sqrt{6}}{360}$	$\frac{296-169\sqrt{6}}{1800}$	$\frac{-2+3\sqrt{6}}{225}$
$\frac{4+\sqrt{6}}{10}$	$\frac{296+169\sqrt{6}}{1800}$	$\frac{88+7\sqrt{6}}{360}$	$\frac{-2-3\sqrt{6}}{225}$
1	$\frac{16-\sqrt{6}}{36}$	$\frac{16+\sqrt{6}}{36}$	$\frac{1}{9}$
	$\frac{16-\sqrt{6}}{36}$	$\frac{16+\sqrt{6}}{36}$	$\frac{1}{9}$

Chapter 3

Trajectory-Based Model Reduction in Chemical Kinetics via Numerical Optimization

In this chapter a historical overview concerning the trajectory-based optimization approach for model reduction in chemical kinetics is given. This optimization problem wants to identify a SIM $\mathcal{W}_\varepsilon$ via minimization of an objective function including information about the course of trajectories. The identification of a SIM results from computing points that lie on or at least near a SIM by using this optimization approach. Therefore, special variables (*reaction progress variables*) are fixed at a special point of time (SIM parameterization) and the optimization problem computes the values of the other free variables at this time in a way that the corresponding point lies on or at least near the SIM. This procedure is called *species reconstruction* and represents a function (cf. z_ε in Theorem 2.1.7) mapping such reaction progress variables onto the full species composition by determining a point on the SIM.

This novel concept for model reduction in chemical kinetics has been introduced in [22] by Lebiedz. The concept can be interpreted as a minimization of relaxing (chemical) forces along reaction trajectories. As relaxation criterion Lebiedz used entropy production (see Subsection 3.2.1) but the results with this criterion have not been satisfying. The next step has been the idea that force and curvature are closely related as, for example, it can be seen in Newton's second law $F = ma = m\ddot{x}$. The interpretation of the novel concept is the minimization of chemical forces and this is why other relaxation criteria – based on the concept of curvature – have been developed and tested over time (see [23, 24, 26, 28, 32, 33, 43]).

In the first section the *optimization approach* is introduced followed by the presentation of different relaxation criteria.

3.1 Optimization Approach

As mentioned in the introduction, Slow Invariant attracting Manifolds (SIMs) are present in the phase space of the dynamical systems considered in this work. These SIMs can be described by a solution of the initial value problem

$$\begin{aligned} \frac{\mathrm{d}c(t)}{\mathrm{d}t} &= f\left(c(t)\right), \quad c(t) \in \mathbb{R}^n \\ c(0) &= c^0 \end{aligned}$$

for special initial values $c(0) = c^0$. For the computation of those initial values the following optimization problem has been developed. Up to now, the general trajectory-based optimization approach was formulated as

$$\min_{c(t)} \int_0^{t_\mathrm{f}} \Phi\left(c(t)\right) \, \mathrm{d}t \tag{3.1a}$$

subject to

$$\frac{\mathrm{d}c(t)}{\mathrm{d}t} = f\left(c(t)\right) \tag{3.1b}$$

$$0 = g\left(c(0)\right) \tag{3.1c}$$

$$c_j(0) = c_j^0, \quad j \in I_\mathrm{fixed}. \tag{3.1d}$$

The variable $c(t) = (c_i(t))_{i=1}^n$ denotes the state vector which contains the concentrations of the chemical species. The objective function is defined in (3.1a) wherein $\Phi\left(c(t)\right)$ is used, describing the optimization criterion related to the degree of relaxation of chemical forces. The time t_f has been chosen large enough so that the final point of integration (final state) is close to equilibrium. System dynamics (e.g. chemical kinetics determined by the reaction mechanism) are described in Equation (3.1b) and enter the optimization problem as equality constraints. Hence, an optimal solution of (3.1) always satisfies the system dynamics of the full ODE system and therefore represents a solution trajectory of (3.1b). Up to now, it has not been assumed that there exists a diffeomorphism in a way that the system (3.1b) can be rewritten as a singular perturbed system (2.2). Additional constraints (e.g. chemical element mass conservation relations in the case of chemical kinetics that have to be obeyed due to the law of mass conservation) are collected in the function g in (3.1c). The index set I_fixed contains the indices of state variables (denoted as *reaction progress variables*) with fixed values at time $t = 0$ chosen to parameterize the reduced model i.e. the slow attracting manifold to be computed. Thus, those state variables representing the actual degrees of freedom within the optimization problem are $c_j(0)$, $j \notin I_\mathrm{fixed}$. The process of determining $c_j(0)$, $j \notin I_\mathrm{fixed}$ from c_j^0, $j \in I_\mathrm{fixed}$ is known as *species reconstruction* and represents a function, mapping the reaction progress variables to the full

species composition by determining a point on the attracting SIM. State variables that are chosen to parameterize the reduced model (SIM) are fixed via the equality constraint (3.1d) at $t = 0$ (fixation of the *reaction progress variables*). The choice of the reaction progress variables is dependent on a detailed knowledge of the chemical mechanism. However, the approach is not restricted to a particular choice.

3.2 Relaxation Criteria

In the next two subsections different ideas for choosing the criterion $\Phi\left(c(t)\right)$ are presented which in general should fulfill the following requirements:

- Φ should describe the extent of relaxation of "chemical forces" in the evolution of reaction trajectories towards equilibrium.
- Φ should be computable from easily accessible data.
- Φ should be twice continuously differentiable along reaction trajectories.

Another property is the *consistency* which is desirable but not necessary:

Definition 3.2.1
Suppose an optimal trajectory $\tilde{c}(t)$ has been computed as a solution of (3.1). Take the concentrations of the reaction progress variables at some time $t_1 > 0$ as new initial concentrations and solve (3.1) again. If the resulting trajectory $\hat{c}(t)$ is equal to the part of the original trajectory that starts from t_1 (i.e. $\hat{c}(t) = \tilde{c}(t + t_1)$) the optimization criterion Φ is called consistent*. Otherwise it is called* inconsistent*.*

The consistency property is visualized in Figure 3.1: The blue circle represents an optimal solution of the optimization problem (3.1). The point which is represented by a black circle is the solution computed with a consistent criterion and the red circle denotes a solution computed with an inconsistent criterion.

Later the solutions of the optimization problem are called consistent/inconsitent which is to say the solutions are computed with an consistent/inconsistent criterion. This consistency property measures the invariance of the manifolds and it is chosen in this way because SIMs are attractve – regardless of their dimensions. This means that trajectories starting from arbitrary initial values converge towards the SIM and once a trajectory is ε-close to the SIM it stays there.

The aim of finding a consistent criterion (i.e. the resulting solution of the optimization problem identifies the SIM exactly) characterizing the SIM is one of the main tasks concerning the trajectory-based optimization approach. Below different criteria are presented which have been tested by various authors [22, 26, 32, 33, 43].

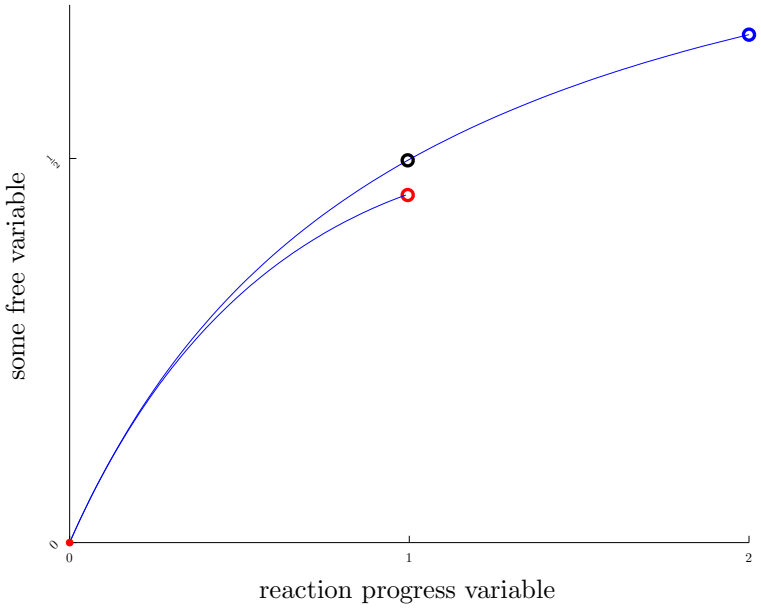

Figure 3.1: Visualization of the consistency property: The blue circle denotes an optimal solution of the optimization problem (3.1), the black circle denotes a solution computed with a consistent criterion, and the red circle a solution computed with an inconsistent criterion.

To compare these criteria with each other the numerical solutions of one chemical mechanism including six species (see Table 3.1) have computed with different criteria by the author. These results can be seen in Figures 3.2–3.3.

Table 3.1: Model hydrogen combustion reaction mechanism with constant reaction rates including six species.

Reaction			k_+	k_-
H_2	$\rightleftharpoons$	$2\,H$	2.0	216.0
O_2	$\rightleftharpoons$	$2\,O$	1.0	337.5
H_2O	$\rightleftharpoons$	$H + OH$	1.0	1400.0
$H_2 + O$	$\rightleftharpoons$	$H + OH$	1000.0	10800.0
$O_2 + H$	$\rightleftharpoons$	$O + OH$	1000.0	33750.0
$H_2 + O$	$\rightleftharpoons$	H_2O	100.0	0.7714

The kinetic model (ODE system) corresponding to the mechanism given in Table 3.1 is given via the law of mass action kinetics (see [3, 41]) by

$$\begin{aligned}
\frac{\mathrm{d}c_{\mathrm{H_2}}}{\mathrm{d}t} &= -k_1 c_{\mathrm{H_2}} + k_{-1} c_{\mathrm{H_2}}^2 - k_4 c_{\mathrm{H_2}} c_{\mathrm{O}} + k_{-4} c_{\mathrm{H}} c_{\mathrm{OH}} \\
&\quad - k_6 c_{\mathrm{H_2}} c_{\mathrm{O}} + k_{-6} c_{\mathrm{H_2O}} \\
\frac{\mathrm{d}c_{\mathrm{H}}}{\mathrm{d}t} &= 2k_1 c_{\mathrm{H_2}} - 2k_{-1} c_{\mathrm{H_2}}^2 + k_3 c_{\mathrm{H_2O}} - k_{-3} c_{\mathrm{H}} c_{\mathrm{OH}} \\
&\quad + k_4 c_{\mathrm{H_2}} c_{\mathrm{O}} - k_{-4} c_{\mathrm{H}} c_{\mathrm{OH}} - k_5 c_{\mathrm{O_2}} c_{\mathrm{H}} + k_{-5} c_{\mathrm{O}} c_{\mathrm{OH}} \\
\frac{\mathrm{d}c_{\mathrm{O_2}}}{\mathrm{d}t} &= -k_2 c_{\mathrm{O_2}} + k_{-2} c_{\mathrm{O}}^2 - k_5 c_{\mathrm{H}} c_{\mathrm{O_2}} + k_{-5} c_{\mathrm{O}} c_{\mathrm{OH}} \\
\frac{\mathrm{d}c_{\mathrm{O}}}{\mathrm{d}t} &= 2k_2 c_{\mathrm{O_2}} - 2k_{-2} c_{\mathrm{O}}^2 - k_4 c_{\mathrm{H_2}} c_{\mathrm{O}} + k_{-4} c_{\mathrm{H}} c_{\mathrm{OH}} \\
&\quad + k_5 c_{\mathrm{H}} c_{\mathrm{O_2}} - k_{-5} c_{\mathrm{O}} c_{\mathrm{OH}} - k_6 c_{\mathrm{H_2}} c_{\mathrm{O}} + k_{-6} c_{\mathrm{H_2O}} \\
\frac{\mathrm{d}c_{\mathrm{H_2O}}}{\mathrm{d}t} &= -k_3 c_{\mathrm{H_2O}} + k_{-3} c_{\mathrm{H}} c_{\mathrm{OH}} + k_6 c_{\mathrm{H_2}} c_{\mathrm{O}} - k_{-6} c_{\mathrm{H_2O}} \\
\frac{\mathrm{d}c_{\mathrm{OH}}}{\mathrm{d}t} &= k_3 c_{\mathrm{H_2O}} - k_{-3} c_{\mathrm{H}} c_{\mathrm{OH}} + k_4 c_{\mathrm{H_2}} c_{\mathrm{O}} - k_{-4} c_{\mathrm{H}} c_{\mathrm{OH}} \\
&\quad + k_5 c_{\mathrm{H}} c_{\mathrm{O_2}} - k_{-5} c_{\mathrm{O}} c_{\mathrm{OH}}.
\end{aligned}$$

This mechanism has also been used in the diploma thesis of Miriam Winkler [43] and in the dissertation of Volkmar Reinhardt [32]. The conservation relations are given by

$$\begin{aligned}
2c_{\mathrm{H_2}} + 2c_{\mathrm{H_2O}} + c_{\mathrm{H}} + c_{\mathrm{OH}} &= 2.0 \\
2c_{\mathrm{O_2}} + c_{\mathrm{H_2O}} + c_{\mathrm{O}} + c_{\mathrm{OH}} &= 1.0.
\end{aligned}$$

With these mass conservation equations – which enter the optimization problem (3.1) in Equation (3.1c) – the system has four degrees of freedom.

3.2.1 Entropy Production

The first criterion was presented by Lebiedz in [22]. In his model reduction approach a special trajectory (called *Minimal Entropy Production Trajectory (MEPT)*) is computed by minimizing the sum of the entropy production rates of single reaction steps. The optimization criterion Φ of the general optimization problem (3.1) is chosen as

$$\Phi\left(c(t)\right) = \sum_{j=1}^{m} \frac{\mathrm{d}S_j}{\mathrm{d}t} \tag{3.2}$$

with $\mathrm{d}S_j/\mathrm{d}t = R(R_{j\rightarrow} - R_{j\leftarrow}) \ln\left(R_{j\rightarrow}/R_{j\leftarrow}\right)$ and R being the gas constant ($R = 8.314472\,\mathrm{J/(K \cdot mol)}$). The notations $R_{j\rightarrow}$ and $R_{j\leftarrow}$ denote the forward

and backward reaction rates for an elementary reaction step j and $\mathrm{d}S_j/\mathrm{d}t$ is the entropy production rate for reaction j.

In Figure 3.2 the results of the optimization problem (3.1) including the entropy production (3.2) as criterion are shown. Therefore different optimization problems – including different values of the reaction progress variables – have been solved. By reason of better visualization the six-dimensional phase space can be seen in five two-dimensional plots (the reaction progress variable is plotted against the other free variables). The blue curves are the trajectories integrated numerically starting at the blue circles which represent the solutions of the optimization problems. The red dot represents the chemical equilibrium. The final time t_f has been chosen 'large enough' for the trajectory to be close to the equilibrium point.

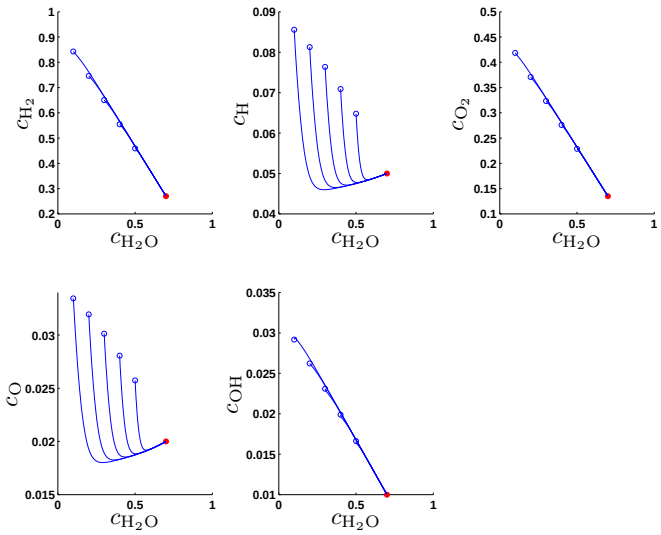

Figure 3.2: Results for the optimization problem (3.1) by using the *entropy production* (3.2) as criterion. The final time t_f is fixed at $t_\mathrm{f} = 1.0$ and $c_{\mathrm{H_2O}}$ is chosen as reaction progress variable.

Obviously one can see that the solutions are inconsistent (mainly in the second (c_H) and in the fourth (c_O) plot). Thus, other relaxation criteria have been developed in order to find one characterizing the SIM (approximately) exactly.

3.2.2 Curvature-Based Relaxation Criteria

As stated above the novel concept for model reduction can be interpreted as a minimization of relaxing forces along reaction trajectories. From the opposite point of view this means that chemical forces are maximally relaxed along trajectories on the attracting SIM. This is why Φ should characterize the relaxation of chemical forces.

From physics it is well-known that the geometric interpretation of a force is closely related to curvature. This can be seen in Newton's second law $F = \dot{p}(t)$ with $p(t) = m(t)\dot{x}(t)$ for example. Here F denotes the force, p the momentum, m the mass, and $\dot{x}$ the velocity. With a temporally constant mass this leads to the following expression:

$$F = m\ddot{x} = ma.$$

In this equation it can be seen that force is closely related to the acceleration a which is equal to the second derivative of the state vector $x(t)$ with respect to time t. The acceleration contains information about the curvature of $x(t)$ and thus Newton's second law describes a relation between force and curvature.

Next a relaxation criteria is presented based on this concept of "force $\approx$ curvature".

Euclidean Norm

To obtain a curvature-based objective function the principle of "force $\approx$ curvature" is transferred to chemical systems. In dissipative ODE systems modeling chemical reaction kinetics the phase flow generally causes anisotropic volume contraction due to multiple time scales with spectral gaps. This force relaxation leads to a change of the reaction velocity (in the context of chemical kinetics). Inspired by Newton's geometric interpretation of a force being the second derivative of the state vector with respect to time, the second time-derivative of the chemical composition $c(t)$ characterizing the rate of change of reaction velocity through relaxation (dissipation) of chemical forces is regarded:

$$\dot{c} = f(c), \quad \ddot{c} = \frac{\mathrm{d}\dot{c}}{\mathrm{d}t} = \frac{\mathrm{d}\dot{c}}{\mathrm{d}c} \cdot \frac{\mathrm{d}c}{\mathrm{d}t} = J_f(c) \cdot f. \tag{3.3}$$

The relaxation of chemical forces results in a change of $\dot{c}(t)$ along a reaction trajectory on its way towards chemical equilibrium. This change can be characterized by taking the directional derivative of the tangent vector of the curve $c(t)$ with respect to its own direction $v := \dot{c}/\|\dot{c}\|_2 = f/\|f\|_2$. Analytically this can be formulated as

$$D_v\dot{c}(t) := \frac{\mathrm{d}}{\mathrm{d}\alpha} f(c(t) + \alpha v)\bigg|_{\alpha=0} = J_f(c) \cdot \frac{f}{\|f\|_2},$$

with $J_f(c)$ being the Jacobian of f evaluated at $c(t)$ and $\|\cdot\|_2$ denoting the Euclidean norm. Hence the preliminary optimization criterion is chosen as

$$\tilde{\Phi}(c) = \frac{\|J_f(c) \cdot f\|_2}{\|f\|_2}. \tag{3.4}$$

The natural way for the evaluation of criterion (3.4) in the formulation of the objective function (3.1a) would be a path integral along the trajectory towards equilibrium

$$\int_{l(0)}^{l(t_\mathrm{f})} \tilde{\Phi}\left(c\left(l(t)\right)\right) \,\mathrm{d}l(t)$$

with $l(t)$ being the Euclidean length of the curve $c(t)$ at time t given by

$$l(t) = \int_0^t \|\dot{c}(\tau)\|_2 \,\mathrm{d}\tau.$$

This results in the reparameterization

$$\mathrm{d}l(t) = \|\dot{c}(t)\|_2 \,\mathrm{d}t.$$

Then the objective function used in (3.1a) is (using (3.3)):

$$\int_0^{t_\mathrm{f}} \Phi\left(c(t)\right) \,\mathrm{d}t = \int_0^{t_\mathrm{f}} \tilde{\Phi}\left(c(t)\right) \|\dot{c}(t)\|_2 \,\mathrm{d}t = \int_0^{t_\mathrm{f}} \|J_f(c) \cdot f\|_2 \,\mathrm{d}t = \int_0^{t_\mathrm{f}} \|\ddot{c}\|_2 \,\mathrm{d}t. \tag{3.5}$$

Figure 3.3 shows the results using $\Phi\left(c(t)\right) = \|J_f(c) \cdot f\|_2$ as relaxation criterion. In comparison to the entropy production as objective function the curvature-based relaxation criterion measured in the Euclidean norm yields better results. But the results are not invariant and so additional relaxation criteria have been tested in [26, 32], which still do not give significantly better results in the fomulation of the general optimization problem (3.1): All points do not lie on the invariant SIM exactly.

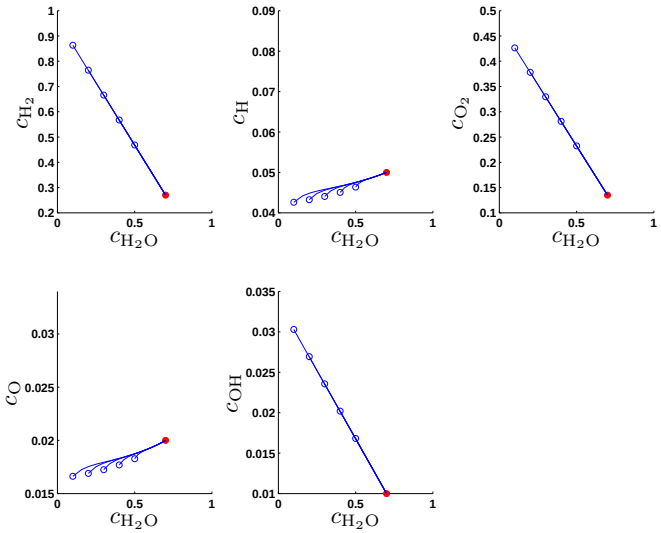

Figure 3.3: Results for the optimization problem (3.1) by using the objective function (3.5). The final time t_f is fixed at $t_f = 1.0$ and the c_{H_2O} is chosen as reaction progress variable.

Chapter 4

Results

In the first section of this chapter a new formulation of the optimization problem (3.1) called *reverse mode* is introduced. This formulation is based on an idea of Dirk Lebiedz. Subsequently theoretical and numerical results are presented for different models. For a two-dimensional linear system and a common non-linear test problem (Davis–Skodje) it is analytically shown that the reverse mode optimization approach asymptotically identifies the SIM $\mathcal{W}_\varepsilon$ exactly in the limit of both an infinite time horizon of the optimization problem with fixed spectral gap of the dynamical system and infinite spectral gap with a fixed finite time horizon. This is the central part of this thesis. Numerical results for linear and non-linear (Davis–Skodje and Semenov) problems as well as more realistic higher-dimensional chemical reaction mechanisms are presented. This new formulation as well as theoretical and numerical results concerning the *reverse mode* formulation can also be found in [27]. Numerical results are obtained by adapting a code – which has been developed by Jochen Siehr – to the mechanisms treated in this thesis.

In the linear model as well as in the Davis–Skodje model the state variables are denoted as $x(t)$ whereas $\big(x(t), y(t)\big)^T$ is used as state vector in the Semenov model.

4.1 New Formulation of the Optimization Approach

The dynamical systems considered in this work can be written as

$$\dot{c}(t) = f\left(c(t)\right), \quad c(t) \in \mathbb{R}^n \tag{4.1}$$

where either the system (4.1) has a singular perturbation form

$$\dot{c}_\mathrm{f} = \quad f_1\left(c_\mathrm{f}, c_\mathrm{s}; \varepsilon\right), \quad c_\mathrm{f}(t) \in \mathbb{R}^{n_\mathrm{f}} \tag{4.2a}$$

$$\dot{c}_\mathrm{s} = \varepsilon f_2\left(c_\mathrm{f}, c_\mathrm{s}; \varepsilon\right), \quad c_\mathrm{s}(t) \in \mathbb{R}^{n_\mathrm{s}} \tag{4.2b}$$

or it is assumed that there exists a diffeomorphism in a way that the system (4.1) can be rewritten as a singular perturbed system (4.2). Furthermore, the phase space of the dynamical systems considered in this thesis involves SIMs $\mathcal{W}_\varepsilon$ which can be expressed as the graph of a function $z_\varepsilon(c_\mathrm{s};\varepsilon)$.

To enhance the accuracy of approximation to SIMs $\mathcal{W}_\varepsilon$ the optimization problem (3.1) has been modified and this adapted version can be formulated as

$$\min_{c_\mathrm{f}(t)} \int_{t_0}^{t_\mathrm{f}} \Phi\left(\left(c_\mathrm{f}(t), c_\mathrm{s}(t)\right)^T\right) \mathrm{d}t \tag{4.3a}$$

subject to

$$\dot{c}_\mathrm{f}(t) = \quad f_1\left(c_\mathrm{f}(t), c_\mathrm{s}(t);\varepsilon\right) \tag{4.3b}$$

$$\dot{c}_\mathrm{s}(t) = \varepsilon f_2\left(c_\mathrm{f}(t), c_\mathrm{s}(t);\varepsilon\right) \tag{4.3c}$$

$$0 = g\left(\left(c_\mathrm{f}(t_*), c_\mathrm{s}(t_*)\right)^T\right) \tag{4.3d}$$

$$c_\mathrm{s}(t_*) = c_\mathrm{s}^{t_*}, \quad c_\mathrm{s} \in K \tag{4.3e}$$

with $t_0 \leqslant t_* \leqslant t_\mathrm{f}$ and $K \subset \mathbb{R}^{n_\mathrm{s}}$ being a compact domain. In this chapter the criterion

$$\Phi\left(\begin{pmatrix} c_\mathrm{f}(t) \\ c_\mathrm{s}(t) \end{pmatrix}\right) = \left\| \begin{pmatrix} J_{f_1}\left(c_\mathrm{f}(t), c_\mathrm{s}(t);\varepsilon\right) \\ J_{f_2}\left(c_\mathrm{f}(t), c_\mathrm{s}(t);\varepsilon\right) \end{pmatrix} \cdot \begin{pmatrix} f_1\left(c_\mathrm{f}(t), c_\mathrm{s}(t);\varepsilon\right) \\ f_2\left(c_\mathrm{f}(t), c_\mathrm{s}(t);\varepsilon\right) \end{pmatrix} \right\|_2^2 \tag{4.4}$$

is used for all mechanisms (except for the results computed with the entropy production). Here, $J_{f_i}\left(c_\mathrm{f}(t), c_\mathrm{s}(t);\varepsilon\right)$ denotes the derivative of $f_i,\ i = 1, 2$ w.r.t. $c(t) = \left(c_\mathrm{f}(t), c_\mathrm{s}(t)\right)^T$. Criterion (4.4) is very similar to the criterion given in Equation (3.5) with the small modification of squaring the Euclidean norm. This modification does not change the solutions of the optimization problem remarkably, but it simplifies further analysis.

The choice of the reaction progress variables is no longer arbitrary in the formulation (4.3), but it is determined by the splitting up of the state variable $c(t)$ into fast ($c_\mathrm{f}(t)$) and slow ($c_\mathrm{s}(t)$) variables: The slow variables c_s are the reaction progress variables and parameterize the SIM $\mathcal{W}_\varepsilon$. It has to be mentioned here that this is not absolutely necessary, since the optimization problem delivers also results for another choice of the reaction progress variables (see e.g. Subsection 4.3.2). However, if the slow variables are known, such variables are chosen to be the reaction progress variables because model reduction wants to describe the long-term dynamics of the system and this is why the slow variables should parameterize the SIM $\mathcal{W}_\varepsilon$.

In previous publications [22, 25, 26, 33] the general optimization problem (4.3) has been formulated with $t_* = t_0 = 0$ and for the numerical computations t_f has been chosen 'large enough' for the trajectory to be close to the chemical equilibrium point. The numerical value $t_0 = 0$ is chosen arbitrary as the used ODE systems are autonomous. Additionally, in contrast to the *forward formulation* in the present chapter the *backward formulation* $t_* = t_\mathrm{f}$ $(= 0)$ is used. In fact this is the more natural formulation for the identification of a trajectory on the SIM which stays on this manifold during backward time evolution. The first case with $t_* = t_0 = 0$ is referred to as the *forward mode* and the latter $(t_* = t_\mathrm{f} = 0)$ as the *reverse mode*. Both modes can be seen as special cases of the general formulation (4.3).

4.2 Linear Model

A very simple two-dimensional linear model is given by the following singular perturbation problem

$$\frac{\mathrm{d}y_1(t)}{\mathrm{d}t} = -\lambda y_1(t) \tag{4.5a}$$

$$\varepsilon\frac{\mathrm{d}y_2(t)}{\mathrm{d}t} = (-\varepsilon\lambda - 1 + \varepsilon)y_2(t) \tag{4.5b}$$

which is written as a slow system (2.3) (y_1 equates to the slow variable c_s and y_2 to the fast one c_f). Here it has to be mentioned that the time t in (4.5) equates to the rescaled time τ in the formulation (2.3). Furthermore, $0 < \varepsilon \ll 1$ and $\lambda > 0$. In the further course of this section as well as in Subsection 4.3.1 and 4.3.2 the time t will always denote this rescaled time τ. By defining $\gamma := \frac{1}{\varepsilon} - 1$ the system (4.5) can be rewritten as

$$\dot{y}_1(t) = -\lambda y_1(t) \tag{4.6a}$$

$$\dot{y}_2(t) = (-\lambda - \gamma)\, y_2(t) \tag{4.6b}$$

where $\gamma > 0$ measures the spectral gap (stiffness) of the system (the stiffness of the model grows with γ). The system matrix B (see (4.7)) defines two eigenspaces: The fast eigenspace Λ_f (corresponding to the eigenvalue $-(\lambda + \gamma)$) and the slow eigenspace Λ_s (corresponding to the eigenvalue $-\lambda$). In linear models the SIM is given by the eigenspace of the slowest eigenvalue.

In Figure 4.1 the vector field of the linear model (4.6) is plotted for two different values of γ: The first case is referred to $\gamma = 1.0$ and the second case to $\gamma = 9.0$. It is easy to see that the slow eigenspace Λ_s (red line) (here equal to the SIM $\mathcal{W}_\varepsilon$) of the second case is much more attractive than the slow eigenspace (SIM) of the first case.

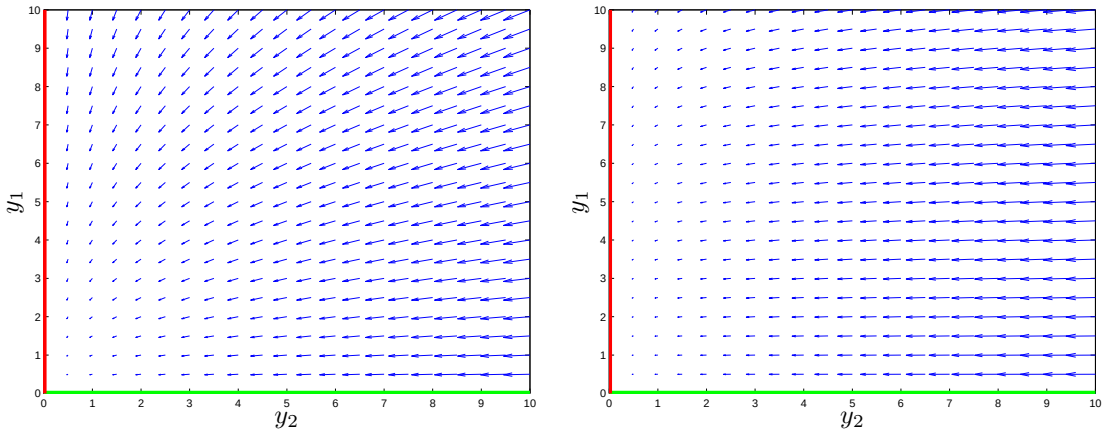

(a) $\gamma = 1.0$ (b) $\gamma = 9.0$

Figure 4.1: Vector fields of System (4.6) for two different values of γ. In both cases λ is chosen as $\lambda = 1$. The green line shows the fast eigenspace Λ_f and the red line the slow one Λ_s (here the SIM is the slow eigenspace).

By using a rotation matrix $R = \begin{pmatrix} \cos\alpha & -\sin\alpha \\ \sin\alpha & \cos\alpha \end{pmatrix}$ and $y(t) = R^{-1}x(t)$, the System (4.6) is transformed to $\dot{x}(t) = RBR^{-1}x(t)$ with

$$B = \begin{pmatrix} -\lambda & 0 \\ 0 & -\lambda - \gamma \end{pmatrix}. \tag{4.7}$$

By using $\alpha = \frac{\pi}{4}$ for example, the matrix $A := RBR^{-1}$ yields

$$\tilde{A} := \begin{pmatrix} -\lambda - \frac{\gamma}{2} & \frac{\gamma}{2} \\ \frac{\gamma}{2} & -\lambda - \frac{\gamma}{2} \end{pmatrix}. \tag{4.8}$$

Thus the SIM $\mathcal{W}_\varepsilon$ (slow eigenspace) is the first bisectrix $x_1 \equiv x_2$ (i.e. $\mathcal{W}_\varepsilon = \{(x_1, x_2) \in \mathbb{R}^2 \mid x_1 = h_\varepsilon(x_2) = x_2,\ x_1 \in K\}$).

In Figure 4.2 the vector fields of the linear model $\dot{x}(t) = \tilde{A}x(t)$ with $\tilde{A}$ as in (4.8) (i.e. $\alpha = \frac{\pi}{4}$) are shown again for two different values of γ. Again one can see that the SIM in Figure 4.2(b) is much more attractive than the SIM in Figure 4.2(a), which is caused by the different values of γ and so by the spectral gap of the system.

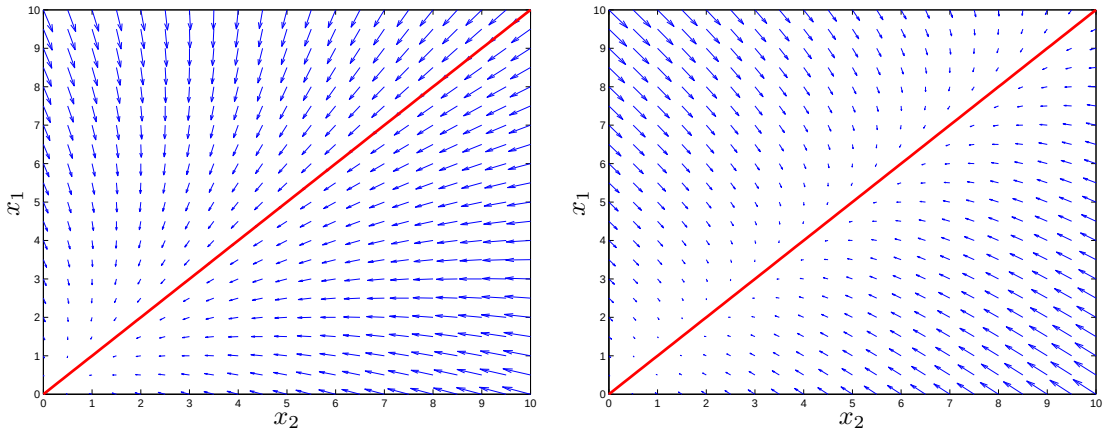

(a) $\gamma = 1.0$ (b) $\gamma = 9.0$

Figure 4.2: Vector fields of System $\dot{x}(t) = \tilde{A}x(t)$ with $\alpha = \frac{\pi}{4}$ for two different values of γ. In both cases λ is chosen as $\lambda = 1$. The red line shows the slow eigenspace Λ_s (i.e. the SIM).

Theoretical Results

One of the central results of this thesis is the proof of the following conjecture of Dirk Lebiedz:

Theorem 4.2.1
Let $\dot{x}(t) = \big(\dot{x}_1(t), \dot{x}_2(t)\big)^T = \tilde{A}x(t)$ be a two-dimensional linear model, $\tilde{A}$ as in (4.8) with distinct (real-valued) eigenvalues $-(\lambda+\gamma)$ and $-\lambda$, $\gamma, \lambda \in \mathbb{R}^+$, fast and slow eigenspaces Λ_f and Λ_s corresponding to $-(\lambda+\gamma)$ and $-\lambda$, respectively. Let x^* be the optimal solution of

$$\begin{aligned} &\min_{x(t)} \int_{t_0}^{t_\mathrm{f}} \left\| \tilde{A}\tilde{A}x(t) \right\|_2^2 \, dt \\ s.t. \qquad &\dot{x}(t) = \tilde{A}x(t) \\ &x_i(t_\mathrm{f}) = x_i^{t_\mathrm{f}}, \quad \textit{either } i = 1 \textit{ or } i = 2. \end{aligned}$$

Then for all $\gamma > 0$, $\lambda > 0$, and $t_0 < t_\mathrm{f}$ it holds

$$\lim_{t_0 \to -\infty} \inf_{b \in \Lambda_\mathrm{s}} \|x^*(t_\mathrm{f}) - b\|_2 = 0.$$

Proof. Let w.l.o.g. be $\lambda = 1$ and the second variable is chosen as progress variable i.e. $x_2(t_\mathrm{f}) = x_2^{t_\mathrm{f}}$. The objective criterion $\Phi(x(t))$ can be computed as

$$\begin{aligned}\left\|\tilde{A}\tilde{A}x(t)\right\|_2^2 =& (x_1(t))^2\left(1+2\gamma+3\gamma^2+2\gamma^3+\frac{\gamma^4}{2}\right)\\ &+(x_2(t))^2\left(1+2\gamma+3\gamma^2+2\gamma^3+\frac{\gamma^4}{2}\right)\\ &+x_1(t)\,x_2(t)\left(-4\gamma-6\gamma^2-4\gamma^3-\gamma^4\right).\end{aligned} \tag{4.9}$$

The general solution of the ODE $\dot{x} = \tilde{A}x$ is

$$x_1(t) = c_1\mathrm{e}^{-t} + c_2\mathrm{e}^{(-1-\gamma)t} \tag{4.10a}$$

$$x_2(t) = c_1\mathrm{e}^{-t} - c_2\mathrm{e}^{(-1-\gamma)t}. \tag{4.10b}$$

Solution (4.10) is substituted into criterion (4.9) and integration over time yields the objective function

$$\begin{aligned}\int_{t_0}^{t_\mathrm{f}}\left\|\tilde{A}\tilde{A}x(t)\right\|_2^2\,\mathrm{d}t &= \int_{t_0}^{t_\mathrm{f}}\left[2c_1^2\mathrm{e}^{-2t}+\left(2+8\gamma+12\gamma^2+8\gamma^3+2\gamma^4\right)c_2^2\mathrm{e}^{(-1-\gamma)2t}\right]\mathrm{d}t\\ &= c_1^2\left(\mathrm{e}^{-2t_0}-\mathrm{e}^{-2t_\mathrm{f}}\right)-\xi c_2^2\left(\mathrm{e}^{(-1-\gamma)2t_0}-\mathrm{e}^{(-1-\gamma)2t_\mathrm{f}}\right)\end{aligned} \tag{4.11}$$

with $\xi = \frac{2+8\gamma+12\gamma^2+8\gamma^3+2\gamma^4}{-2-2\gamma} < 0$. An expression $c_1(c_2)$ for c_1 as a function of c_2 can be calculated from (4.10b) which only depends on c_2 because of the fixed final value of $x_2(t_\mathrm{f})$:

$$x_2(t_\mathrm{f}) = c_1\mathrm{e}^{-t_\mathrm{f}} - c_2\mathrm{e}^{(-1-\gamma)t_\mathrm{f}} \quad\Longrightarrow\quad c_1(c_2) = \frac{x_2\left(t_\mathrm{f}\right)+c_2\mathrm{e}^{(-1-\gamma)t_\mathrm{f}}}{\mathrm{e}^{-t_\mathrm{f}}}.$$

This formula can be used to eliminate c_1 from (4.11) leading to an expression $h(c_2)$ only depending on c_2 (and t_0, t_f, γ which are assumed to be fixed at the moment)

$$\begin{aligned}h\left(c_2\right) :=& \frac{\left(x_2^{t_\mathrm{f}}\right)^2\mathrm{e}^{-2t_0}}{\mathrm{e}^{-2t_\mathrm{f}}}+\frac{\mathrm{e}^{(-1-\gamma)2t_\mathrm{f}}\mathrm{e}^{-2t_0}}{\mathrm{e}^{-2t_\mathrm{f}}}c_2^2+\frac{2x_2^{t_\mathrm{f}}\mathrm{e}^{(-1-\gamma)t_\mathrm{f}}\mathrm{e}^{-2t_0}}{\mathrm{e}^{-2t_\mathrm{f}}}c_2\\ &-\left(x_2^{t_\mathrm{f}}\right)^2-\mathrm{e}^{(-1-\gamma)2t_\mathrm{f}}c_2^2-2x_2^{t_\mathrm{f}}\mathrm{e}^{(-1-\gamma)t_\mathrm{f}}c_2\\ &-\xi\mathrm{e}^{(-1-\gamma)2t_0}c_2^2+\xi\mathrm{e}^{(-1-\gamma)2t_\mathrm{f}}c_2^2=\int_{t_0}^{t_\mathrm{f}}\left\|\tilde{A}\tilde{A}x(t)\right\|_2^2\,\mathrm{d}t,\end{aligned}$$

which should be minimal for identification of the optimal c_2. The first order necessary condition for a minimum $\frac{\mathrm{d}h(c_2)}{\mathrm{d}c_2} = 0$ gives a solution

$$\hat{c}_2 = \frac{x_2^{t_\mathrm{f}} \mathrm{e}^{(-1-\gamma)t_\mathrm{f}} - x_2^{t_\mathrm{f}} \mathrm{e}^{(1-\gamma)t_\mathrm{f}} \mathrm{e}^{-2t_0}}{\mathrm{e}^{-2\gamma t_\mathrm{f}} \mathrm{e}^{-2t_0} - \xi \mathrm{e}^{(-1-\gamma)2t_0} + (\xi - 1)\mathrm{e}^{(-1-\gamma)2t_\mathrm{f}}}.$$

Checking the second-order sufficient conditions

$$\frac{\mathrm{d}^2 h}{\mathrm{d}c_2^2} \equiv 2\mathrm{e}^{-2\gamma t_\mathrm{f}} \left(\mathrm{e}^{-2t_0} - \mathrm{e}^{-2t_\mathrm{f}}\right) + 2\xi \left(\mathrm{e}^{-2t_\mathrm{f}} \mathrm{e}^{-2\gamma t_\mathrm{f}} - \mathrm{e}^{-2t_0} \mathrm{e}^{-2\gamma t_0}\right) > 0 \quad \forall c_2,\ t_\mathrm{f} > t_0$$

guarantees $\hat{c}_2$ being a minimum.
The solution $\hat{c}_2$ and $c_1(\hat{c}_2)$ are substituted in (4.10a) and evaluated at fixed final time t_f yielding an expression for $x_1(t_\mathrm{f})$ additionally depending on γ and t_0

$$\begin{aligned}
x_1(t_\mathrm{f}) &= c_1(\hat{c}_2)\mathrm{e}^{-t_\mathrm{f}} + \hat{c}_2 \mathrm{e}^{(-1-\gamma)t_\mathrm{f}} = \frac{x_2^{t_\mathrm{f}} + \hat{c}_2 \mathrm{e}^{(-1-\gamma)t_\mathrm{f}}}{\mathrm{e}^{-t_\mathrm{f}}} \mathrm{e}^{-t_\mathrm{f}} + \hat{c}_2 \mathrm{e}^{(-1-\gamma)t_\mathrm{f}} \\
&= x_2^{t_\mathrm{f}} \left[1 + \underbrace{\left(\frac{2\mathrm{e}^{(-1-\gamma)2t_\mathrm{f}} - 2\mathrm{e}^{-2\gamma t_\mathrm{f}} \mathrm{e}^{-2t_0}}{\mathrm{e}^{-2\gamma t_\mathrm{f}} \mathrm{e}^{-2t_0} - \xi \mathrm{e}^{(-1-\gamma)2t_0} + (\xi - 1)\, \mathrm{e}^{(-1-\gamma)2t_\mathrm{f}}} \right)}_{=:\chi} \right] \\
&= x_2^{t_\mathrm{f}} \left[1 + \left(\frac{2\mathrm{e}^{(-1-\gamma)2t_\mathrm{f}}}{\mathrm{e}^{-2\gamma t_\mathrm{f}} \mathrm{e}^{-2t_0} - \xi \mathrm{e}^{(-1-\gamma)2t_0} + (\xi - 1)\, \mathrm{e}^{(-1-\gamma)2t_\mathrm{f}}} \right.\right. \\
&\qquad \left.\left. - \frac{2\mathrm{e}^{-2\gamma t_\mathrm{f}}}{\mathrm{e}^{-2\gamma t_\mathrm{f}} - \xi \mathrm{e}^{-2\gamma t_0} + (\xi - 1)\, \mathrm{e}^{(-1-\gamma)2t_\mathrm{f}} \mathrm{e}^{2t_0}} \right) \right]
\end{aligned} \tag{4.12}$$

with error term χ quantifying the deviation from the slow eigenspace $x_1 \equiv x_2$. Finally in the limit $t_0 \to -\infty$ it can be seen that

$$\lim_{t_0 \to -\infty} x_1(t_\mathrm{f}) = x_2^{t_\mathrm{f}}$$

meaning the slow eigenspace $x_1(t) = x_2(t)$ (i.e. the SIM $\mathcal{W}_\varepsilon = \{(x_1, x_2) \in \mathbb{R}^2 \mid x_1 = h_\varepsilon(x_2) = x_2,\ x_1 \in K\}$) is identified by a solution of the optimization problem. □

In Figure 4.3 the error term χ is plotted. It illustrates that for increasing spectral gap γ and increasing time interval $[t_0, t_\mathrm{f}]$ the approximation of the SIM improves while the approximation error decreases exponentially.

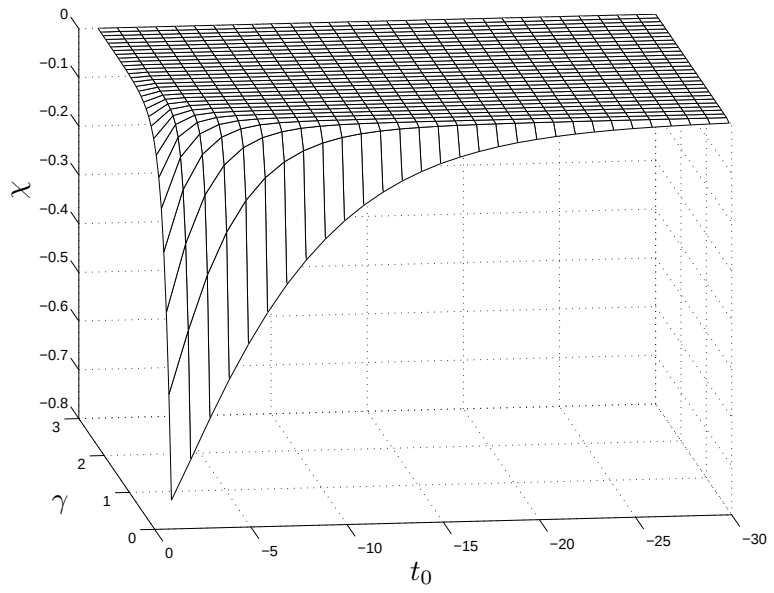

Figure 4.3: The error term χ in (4.12) plotted against t_0 and γ with $t_\mathrm{f} = 0$.

Numerical Results

Figure 4.4 and Figure 4.5 depict numerical solution results of problem (4.3) with the linear model

$$\dot{x}(t) = \begin{pmatrix} -\lambda - \frac{\gamma}{2} & \frac{\gamma}{2} \\ \frac{\gamma}{2} & -\lambda - \frac{\gamma}{2} \end{pmatrix} x(t) \tag{4.13}$$

and small time scale separation $\gamma = 0.2$ and $\gamma = 1.0$ respectively. Solutions for the *forward mode* and the *reverse mode* are shown. Figures 4.4(b)–(f) show five plots computed with the *reverse mode* with different time intervals. In all cases x_2 is chosen as reaction progress variable (parameterization of the SIM $\mathcal{W}_\varepsilon$) and fixed at four different values $x_2^{t_\mathrm{f}} = 2.0,\ 1.5,\ 1.0,\ 0.5$ for each of which the optimization problem is solved to obtain the coordinate of the other variable $x_1(t_\mathrm{f})$ supposed to be located on the SIM. The red curve is the SIM (slow eigenspace) which is given as the first bisectrix ($x_1 = h_\varepsilon(x_2) = x_2$) and the blue curves are the trajectories integrated numerically crossing those points (blue circles) that are computed as solutions of the optimization problem. The red dot represents the equilibrium point (stable fixed point). Obviously the *reverse mode* gives solutions that are significantly closer to the SIM than the *forward mode* (Figure 4.4(a)) and the solutions of the *reverse mode* improve with increasing time interval according to the theoretical results. Figure 4.5 – where a larger spectral gap ($\gamma = 1.0$) is used – shows similar results. Comparing Figure 4.4 and Figure 4.5 one can see that the accuracy of approximation of the SIM improves with increasing spectral gap.

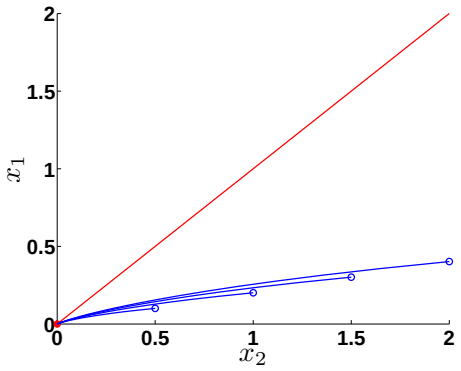

(a) *Forward mode*: $t_0 = 0.0$, $t_\mathrm{f} = 10.0$.

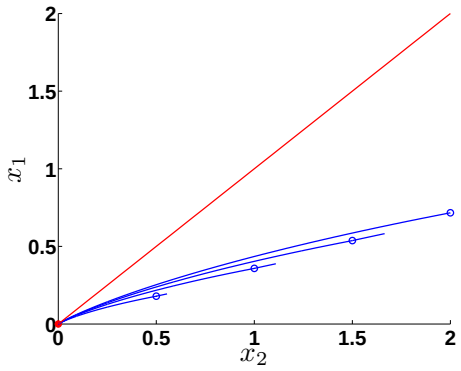

(b) *Reverse mode*: $t_0 = -0.1$, $t_\mathrm{f} = 0.0$.

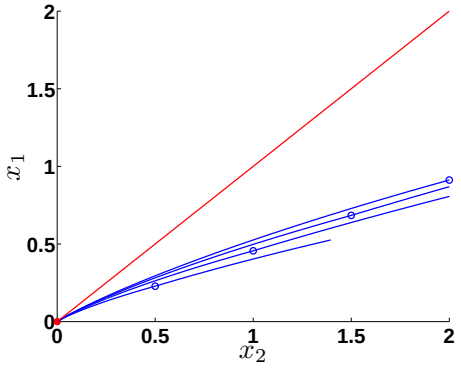

(c) *Reverse mode*: $t_0 = -1.0$, $t_\mathrm{f} = 0.0$.

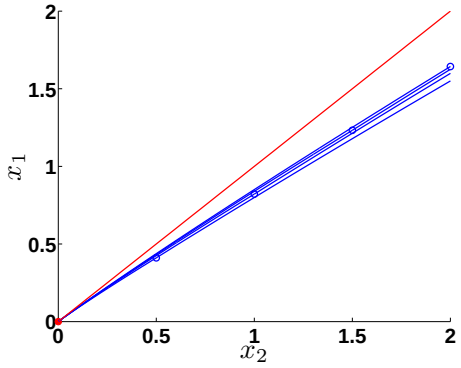

(d) *Reverse mode*: $t_0 = -5.0$, $t_\mathrm{f} = 0.0$.

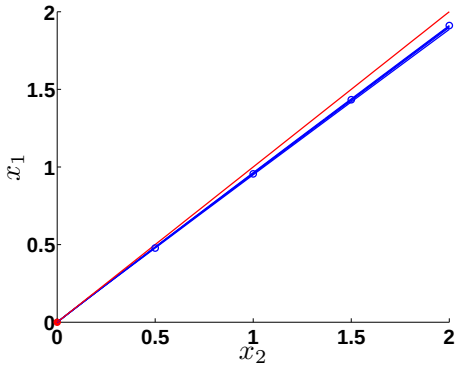

(e) *Reverse mode*: $t_0 = -10.0$, $t_\mathrm{f} = 0.0$.

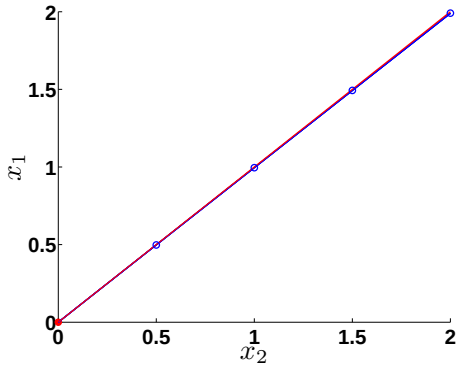

(f) *Reverse mode*: $t_0 = -21.0$, $t_\mathrm{f} = 0.0$.

Figure 4.4: Numerical results for the linear model (4.13) with $\gamma = 0.2$, (a) *forward mode*: $x_2(t_0) = x_2^{t_0}$, and (b), (c), (d), (e) and (f) *reverse mode*: $x_2(t_\mathrm{f}) = x_2^{t_\mathrm{f}}$.

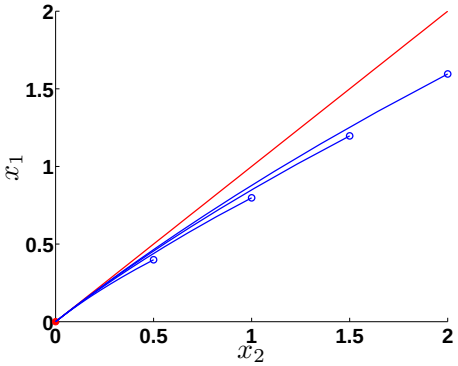

(a) *Forward mode*: $t_0 = 0.0$, $t_\mathrm{f} = 10.0$.

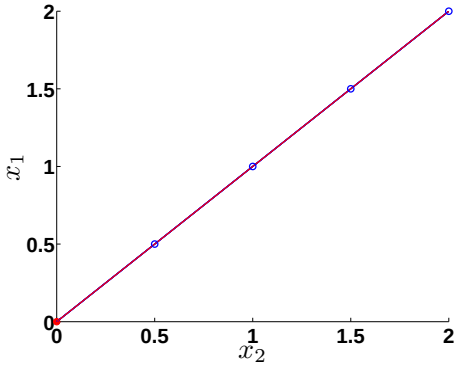

(b) *Reverse mode*: $t_0 = -17.0$, $t_\mathrm{f} = 0.0$.

Figure 4.5: Numerical results for the linear model (4.13) with $\gamma = 1.0$, (a) *forward mode*: $x_2(t_0) = x_2^{t_0}$, and (b) *reverse mode*: $x_2(t_\mathrm{f}) = x_2^{t_\mathrm{f}}$.

4.3 Non-Linear Models

4.3.1 Davis–Skodje Problem

The Davis–Skodje model (4.14) [8, 36] is widely used for analysis and performance tests of model reduction techniques supposed to identify SIMs

$$\frac{\mathrm{d}x_1}{\mathrm{d}t} = -x_1 \tag{4.14a}$$

$$\frac{\mathrm{d}x_2}{\mathrm{d}t} = -\gamma x_2 + \frac{(\gamma-1)x_1 + \gamma x_1^2}{(1+x_1)^2} \tag{4.14b}$$

where $\gamma > 1$ is a measure for the spectral gap (stiffness) of the system. By using $\varepsilon := \frac{1}{\gamma}$ the system has the following singular perturbation form

$$\begin{aligned}\frac{\mathrm{d}x_1}{\mathrm{d}t} &= -x_1 \\ \varepsilon\frac{\mathrm{d}x_2}{\mathrm{d}t} &= -x_2 + \frac{x_1}{1+x_1} - \frac{\varepsilon x_1}{(1+x_1)^2}.\end{aligned}$$

Typically model reduction algorithms show a good performance for large values of γ which represent a large time scale separation. Small values of γ impose a significantly harder challenge on the computation of the SIM $\mathcal{W}_\varepsilon$. For reasons of adjustable time scale separation and analytically computable SIM ($x_2 = h_\varepsilon(x_1) = \frac{x_1}{1+x_1}$) the Davis–Skodje model is widely used for testing numerical model reduction approaches. Analytical and numerical results for the variational approach with the Davis–Skodje model are provided.

Figure 4.6 shows the vector field of the Davis–Skodje problem (4.14) with two different values of γ. Obviously the SIM $\mathcal{W}_\varepsilon$ of the system that includes the spectral gap $\gamma = 10.0 > 2.0$ is much more attractive because of the larger time scale separation.

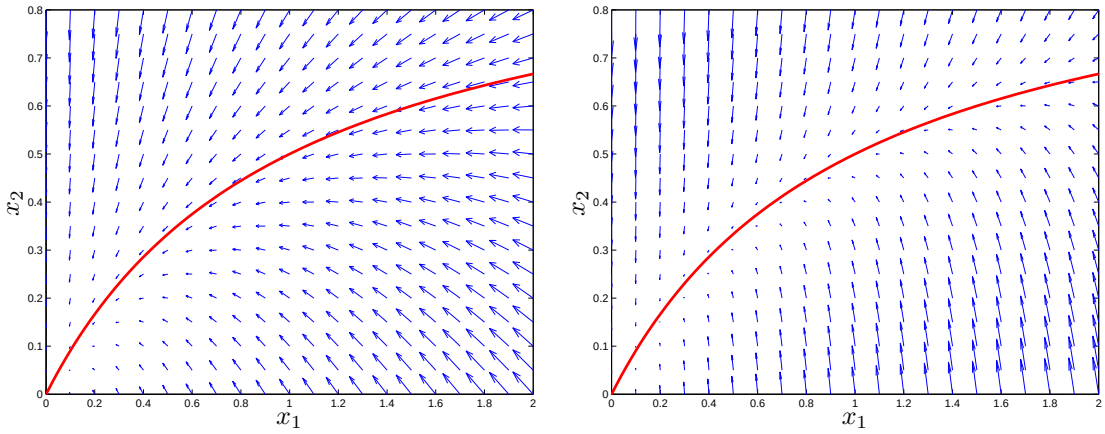

(a) $\gamma = 2.0$ (b) $\gamma = 10.0$

Figure 4.6: Vector fields of System (4.14) for two different values of γ. The red line shows the analytically calculated SIM $\mathcal{W}_\varepsilon = \{(x_1, x_2) \in \mathbb{R}^2 \mid x_2 = h_\varepsilon(x_1) = \frac{x_1}{1+x_1},\ x_1 \in K\}$.

Theoretical Results

Similar results as in the linear case can be obtained for the non-linear Davis–Skodje model.

Theorem 4.3.1
Let $\dot{x}(t) = \left(\dot{x}_1(t), \dot{x}_2(t)\right)^T = \left(f_1\left(x(t)\right), f_2\left(x(t)\right)\right)^T = f\left(x(t)\right)$ *be the Davis–Skodje model (4.14), the slow invariant manifold defined by* $\mathcal{W}_\varepsilon := \{(x_1, x_2) \in \mathbb{R}^2 \mid x_2 = h_\varepsilon(x_1) = \frac{x_1}{1+x_1},\ x_1 \in K\}$, *and* x^* *the optimal solution of*

$$\begin{aligned} \min_{x(t)} & \int_{t_0}^{t_\mathrm{f}} \left\| J_f\left(x(t)\right) \cdot f\left(x(t)\right) \right\|_2^2 \, dt \\ s.t. \quad & \dot{x}(t) = f\left(x(t)\right) \\ & x_1(t_\mathrm{f}) = x_1^{t_\mathrm{f}} \end{aligned}$$

Then for all $\gamma > 1$ *and* $t_0 < t_\mathrm{f}$ *it holds*

$$\lim_{t_0 \to -\infty} \inf_{b \in \mathcal{W}_\varepsilon} \|x^*(t_\mathrm{f}) - b\|_2 = 0.$$

Proof. The Jacobian of f is given by

$$J_f\left(x(t)\right) = \begin{pmatrix} -1 & 0 \\ \dfrac{(1+\gamma)x_1(t)+\gamma-1}{\left(1+x_1(t)\right)^3} & -\gamma \end{pmatrix}.$$

The criterion $\Phi\left(x(t)\right) = \left\| J_f\left(x(t)\right) \cdot f\left(x(t)\right) \right\|_2^2$ in the objective function can be calculated explicitly as

$$\begin{aligned}\Phi\left(x(t)\right) = {} & \left(x_1(t)\right)^2 + \gamma^4 \left(x_2(t)\right)^2 + \frac{\left(x_1(t)\right)^2\left(1-2\gamma^2+\gamma^4\right)}{\left(1+x_1(t)\right)^6} \\ & + \frac{\left(x_1(t)\right)^3\left(-2-2\gamma^2+4\gamma^4\right)}{\left(1+x_1(t)\right)^6} + \frac{\left(x_1(t)\right)^4\left(1+2\gamma^2+6\gamma^4\right)}{\left(1+x_1(t)\right)^6} \\ & + \frac{\left(x_1(t)\right)^5\left(2\gamma^2+4\gamma^4\right)}{\left(1+x_1(t)\right)^6} + \frac{\left(x_1(t)\right)^6\gamma^4}{\left(1+x_1(t)\right)^6} \\ & - x_1(t)x_2(t)\frac{\left(2\gamma^2x_1(t)-2\gamma^2+2\gamma^4+4\gamma^4x_1(t)+2\gamma^4\left(x_1(t)\right)^2\right)}{\left(1+x_1(t)\right)^3}.\end{aligned}$$

An analytical solution of model (4.14) will be computed in the following. The first differential equation yields $x_1(t) = c_1\mathrm{e}^{-t}$ as the general solution. Equation (4.14b) is an inhomogeneous first order linear ODE and the method of variation of constants gives $x_2(t) = x_{2,\mathrm{hom}}(t) + x_{2,\mathrm{part}}(t)$. The homogeneous equation is solved by $x_{2,\mathrm{hom}}(t) = c_2\mathrm{e}^{-\gamma t}$ as $\dot{x}_{2,\mathrm{hom}}(t) = -\gamma c_2\mathrm{e}^{-\gamma t} = -\gamma x_{2,\mathrm{hom}}(t)$. To determine $x_{2,\mathrm{part}}(t)$ the equation

$$\mathrm{e}^{-\gamma t}\dot{c}_2(t) = \frac{(\gamma-1)\,c_1\mathrm{e}^{-t} + \gamma c_1^2\mathrm{e}^{-2t}}{\left(1+c_1\mathrm{e}^{-t}\right)^2}$$

has to be solved for c_2:

$$c_2(t) = \int \dot{c}_2(t)\,\mathrm{d}t = \int \frac{(\gamma-1)\,c_1\mathrm{e}^{-t} + \gamma c_1^2\mathrm{e}^{-2t}}{\mathrm{e}^{-\gamma t}\left(1+c_1\mathrm{e}^{-t}\right)^2}\,\mathrm{d}t = \frac{c_1\mathrm{e}^{\gamma t}}{c_1+\mathrm{e}^t}.$$

Therefore the missing expression is

$$x_{2,\mathrm{part}}(t) = \mathrm{e}^{-\gamma t}\frac{c_1\mathrm{e}^{\gamma t}}{c_1+\mathrm{e}^t} = \frac{c_1}{c_1+\mathrm{e}^t}$$

and the full solution of the ODE is given by

$$x_1(t) = c_1\mathrm{e}^{-t} \tag{4.16a}$$

$$x_2(t) = c_2\mathrm{e}^{-\gamma t} + \frac{c_1}{c_1+\mathrm{e}^t}. \tag{4.16b}$$

Now the criterion Φ is integrated over time using (4.16). In the next formula r_i, $i = 1, 2$ represents a "rest" – all terms independent of $x_2(t)$ hence also independent of c_2 which annihilate after differentiation with respect to c_2 afterwards. Making use of $c_1 = x_1(t_\mathrm{f})\mathrm{e}^{t_\mathrm{f}} = x_1^{t_\mathrm{f}}\mathrm{e}^{t_\mathrm{f}}$ due to (4.16a) yields an expression for the objective function only depending on c_2:

$$\begin{aligned}
h(c_2) :=\ & r_1 + \int_{t_0}^{t_\mathrm{f}} \gamma^4 \left(x_2(t)\right)^2 \,\mathrm{d}t \\
& - \int_{t_0}^{t_\mathrm{f}} x_1(t)x_2(t) \frac{2\gamma^2 x_1(t) - 2\gamma^2 + 2\gamma^4 + 4\gamma^4 x_1(t) + 2\gamma^4 \left(x_1(t)\right)^2}{\left(1 + x_1(t)\right)^3} \,\mathrm{d}t \\
=\ & r_2 + c_2^2 \left(\frac{1}{2}\gamma^3 \mathrm{e}^{-2\gamma t_0} - \frac{1}{2}\gamma^3 \mathrm{e}^{-2\gamma t_\mathrm{f}}\right) \\
& + c_2 \int_{t_0}^{t_\mathrm{f}} \underbrace{\left[\frac{2\gamma^4 c_1 \mathrm{e}^{-\gamma t}}{c_1 + \mathrm{e}^t} - 2\gamma^2 c_1 \mathrm{e}^{(-1-\gamma)t} \frac{c_1 \mathrm{e}^{-t} - 1 + \gamma^2\left(1 + 2c_1\mathrm{e}^{-t} + c_1^2 \mathrm{e}^{-2t}\right)}{(1 + c_1 \mathrm{e}^{-t})^3}\right]}_{=:\varphi(t)} \mathrm{d}t \\
=\ & \int_{t_0}^{t_\mathrm{f}} \left\| J_f\left(x(t)\right) \cdot f\left(x(t)\right)\right\|_2^2 \,\mathrm{d}t.
\end{aligned}$$

The necessary first-order condition for a minimum is applied. Setting $\frac{\mathrm{d}h(c_2)}{\mathrm{d}c_2} = 0$ results in

$$\check{c}_2 := \frac{-\int_{t_0}^{t_\mathrm{f}} \varphi(t)\,\mathrm{d}t}{\gamma^3 \mathrm{e}^{-2\gamma t_0} - \gamma^3 \mathrm{e}^{-2\gamma t_\mathrm{f}}}.$$

The second-order check

$$\frac{\mathrm{d}^2 h}{\mathrm{d}c_2^2} \equiv \gamma^3 \mathrm{e}^{-2\gamma t_0} - \gamma^3 \mathrm{e}^{-2\gamma t_\mathrm{f}} > 0 \quad \forall c_2,\ t_0 < t_\mathrm{f},\ \gamma > 1$$

assures $\check{c}_2$ being a minimum.
An expression for $x_2(t_\mathrm{f})$ can be derived by substituting c_1 and $\check{c}_2$ in (4.16b):

$$x_2\left(t_\mathrm{f}\right) = \frac{-\int_{t_0}^{t_\mathrm{f}} \varphi(t)\,\mathrm{d}t}{\gamma^3 \mathrm{e}^{-2\gamma t_0} - \gamma^3 \mathrm{e}^{-2\gamma t_\mathrm{f}}} \mathrm{e}^{-\gamma t_\mathrm{f}} + \frac{x_1^{t_\mathrm{f}}}{x_1^{t_\mathrm{f}} + 1}.$$

The proof for the relation

$$\lim_{t_0 \to -\infty} \frac{-\int_{t_0}^{t_\mathrm{f}} \varphi(t)\,\mathrm{d}t}{\gamma^3 \mathrm{e}^{-2\gamma t_0} - \gamma^3 \mathrm{e}^{-2\gamma t_\mathrm{f}}} \mathrm{e}^{-\gamma t_\mathrm{f}} = 0 \tag{4.17}$$

will be given in the following Lemma 4.3.2. According to (4.17) it holds

$$\lim_{t_0 \to -\infty} x_2(t_\mathrm{f}) = \frac{x_1^{t_\mathrm{f}}}{x_1^{t_\mathrm{f}} + 1}$$

which is the analytic expression for the SIM $\mathcal{W}_\varepsilon$ of the Davis–Skodje system (see [8]). This completes the proof. □

Lemma 4.3.2
Under the conditions of Theorem 4.3.1 Equation (4.17) holds.

Proof. First the numerator and the denominator of the following expression is denoted by $a(t_0)$ and $b(t_0)$, respectively:

$$\frac{-\int_{t_0}^{t_\mathrm{f}}\varphi(t)\,\mathrm{d}t\mathrm{e}^{-\gamma t_\mathrm{f}}}{\gamma^3\mathrm{e}^{-2\gamma t_0}-\gamma^3\mathrm{e}^{-2\gamma t_\mathrm{f}}} =: \frac{a(t_0)}{b(t_0)}.$$

It holds that $b(t_0)\to\infty$ for $t_0\to-\infty$. For the numerator $a(t_0)$ two cases are possible:

- If $a(t_0)\nrightarrow\pm\infty$ for $t_0\to-\infty$ then $\dfrac{a(t_0)}{b(t_0)}\to 0$ for $t_0\to-\infty$ and (4.17) holds.

- If $a(t_0)\to\pm\infty$ for $t_0\to-\infty$ then l'Hospital's rule is apllied:

$$\frac{\frac{\mathrm{d}}{\mathrm{d}t_0}a(t_0)}{\frac{\mathrm{d}}{\mathrm{d}t_0}b(t_0)} = \frac{\varphi(t_0)\mathrm{e}^{-\gamma t_\mathrm{f}}}{-2\gamma^4\mathrm{e}^{-2\gamma t_0}}. \tag{4.18}$$

  The expression $\varphi(t_0)$ has the following form which is split up into $\varphi_1(t_0)$ and $\varphi_2(t_0)$:

$$\varphi(t_0) = \underbrace{\frac{2\gamma^4 c_1\mathrm{e}^{-\gamma t_0}}{c_1+\mathrm{e}^{t_0}}}_{=:\varphi_1(t_0)} - \underbrace{2\gamma^2 c_1\mathrm{e}^{(-1-\gamma)t_0}\frac{c_1\mathrm{e}^{-t_0}-1+\gamma^2\left(1+2c_1\mathrm{e}^{-t_0}+c_1^2\mathrm{e}^{-2t_0}\right)}{(1+c_1\mathrm{e}^{-t_0})^3}}_{=:\varphi_2(t_0)}.$$

  From Equation (4.18) only the following expression is considered because of dependency on t_0:

$$\frac{\varphi(t_0)}{\mathrm{e}^{-2\gamma t_0}} = \frac{\varphi_1(t_0)}{\mathrm{e}^{-2\gamma t_0}} - \frac{\varphi_2(t_0)}{\mathrm{e}^{-2\gamma t_0}}.$$

  By considering the first term it is not difficult to see the convergence to 0 for $t_0\to-\infty$:

$$\begin{aligned}\frac{\varphi_1(t_0)}{\mathrm{e}^{-2\gamma t_0}} &= \frac{2\gamma^4 c_1\mathrm{e}^{-\gamma t_0}}{(c_1+\mathrm{e}^{t_0})\,\mathrm{e}^{-2\gamma t_0}} = \frac{2\gamma^4 c_1}{(c_1+\mathrm{e}^{t_0})\,\mathrm{e}^{-\gamma t_0}}\\ &= \frac{2\gamma^4 c_1}{c_1\mathrm{e}^{-\gamma t_0}+\mathrm{e}^{(1-\gamma)t_0}} \to 0 \text{ for } t_0\to-\infty.\end{aligned}$$

  The second term requires a little more analysis to show convergence to 0 for $t_0\to-\infty$:

$$\begin{aligned}\frac{\varphi_2(t_0)}{\mathrm{e}^{-2\gamma t_0}} &= 2\gamma^2 c_1\mathrm{e}^{(-1-\gamma)t_0}\frac{c_1\mathrm{e}^{-t_0}-1+\gamma^2\left(1+2c_1\mathrm{e}^{-t_0}+c_1^2\mathrm{e}^{-2t_0}\right)}{(1+c_1\mathrm{e}^{-t_0})^3\mathrm{e}^{-2\gamma t_0}}\\ &= 2\gamma^2 c_1\frac{c_1\mathrm{e}^{-t_0}-1+\gamma^2\left(1+2c_1\mathrm{e}^{-t_0}+c_1^2\mathrm{e}^{-2t_0}\right)}{(1+c_1\mathrm{e}^{-t_0})^3\mathrm{e}^{(1-\gamma)t_0}}.\end{aligned}$$

Hereof only $\frac{\mathrm{e}^{-t_0}}{(1+c_1\mathrm{e}^{-t_0})^3\mathrm{e}^{(1-\gamma)t_0}}$ and $\frac{\mathrm{e}^{-2t_0}}{(1+c_1\mathrm{e}^{-t_0})^3\mathrm{e}^{(1-\gamma)t_0}}$ has to be considered which are denoted by $\Phi_1(t_0)$ and $\Phi_2(t_0)$, respectively. These two terms are considered separately:

$$\lim_{t_0\to-\infty}\Phi_1(t_0) := \lim_{t_0\to-\infty}\frac{\mathrm{e}^{-t_0}}{(1+c_1\mathrm{e}^{-t_0})^3\mathrm{e}^{(1-\gamma)t_0}} = \lim_{t_0\to-\infty}\frac{\mathrm{e}^{(-2+\gamma)t_0}}{(1+c_1\mathrm{e}^{-t_0})^3} = 0$$

$$\iff \lim_{t_0\to-\infty}\frac{(1+c_1\mathrm{e}^{-t_0})^3}{\mathrm{e}^{(-2+\gamma)t_0}} = \infty. \tag{4.19}$$

To prove (4.19) the expression is split up into four terms, which are considered separately for $t_0 \to -\infty$:

$$\begin{aligned}\frac{(1+c_1\mathrm{e}^{-t_0})^3}{\mathrm{e}^{(-2+\gamma)t_0}} &= \frac{1}{\mathrm{e}^{(-2+\gamma)t_0}} + \frac{3c_1\mathrm{e}^{-t_0}}{\mathrm{e}^{(-2+\gamma)t_0}} + \frac{3c_1^2\mathrm{e}^{-2t_0}}{\mathrm{e}^{(-2+\gamma)t_0}} + \frac{c_1^3\mathrm{e}^{-3t_0}}{\mathrm{e}^{(-2+\gamma)t_0}} \\ &= \underbrace{\mathrm{e}^{(2-\gamma)t_0}}_{\to 0,1,\text{or}+\infty} + \underbrace{3c_1\mathrm{e}^{(1-\gamma)t_0}}_{\to+\infty} + \underbrace{3c_1^2\mathrm{e}^{-\gamma t_0}}_{\to+\infty} + \underbrace{c_1^3\mathrm{e}^{(-1-\gamma)t_0}}_{\to+\infty}.\end{aligned}$$

This confirms (4.19) and hence also $\lim_{t_0\to-\infty}\Phi_1(t_0) = 0$.

For the second term $\Phi_2(t_0)$ the same procedure is done:

$$\lim_{t_0\to-\infty}\Phi_2(t_0) := \lim_{t_0\to-\infty}\frac{\mathrm{e}^{-2t_0}}{(1+c_1\mathrm{e}^{-t_0})^3\mathrm{e}^{(1-\gamma)t_0}} = \lim_{t_0\to-\infty}\frac{\mathrm{e}^{(-3+\gamma)t_0}}{(1+c_1\mathrm{e}^{-t_0})^3} = 0$$

$$\iff \lim_{t_0\to-\infty}\frac{(1+c_1\mathrm{e}^{-t_0})^3}{\mathrm{e}^{(-3+\gamma)t_0}} = \infty. \tag{4.20}$$

To prove (4.20) the expression is split up into four terms again, which are considered separately for $t_0 \to -\infty$:

$$\begin{aligned}\frac{(1+c_1\mathrm{e}^{-t_0})^3}{\mathrm{e}^{(-3+\gamma)t_0}} &= \frac{1}{\mathrm{e}^{(-3+\gamma)t_0}} + \frac{3c_1\mathrm{e}^{-t_0}}{\mathrm{e}^{(-3+\gamma)t_0}} + \frac{3c_1^2\mathrm{e}^{-2t_0}}{\mathrm{e}^{(-3+\gamma)t_0}} + \frac{c_1^3\mathrm{e}^{-3t_0}}{\mathrm{e}^{(-3+\gamma)t_0}} \\ &= \underbrace{\mathrm{e}^{(3-\gamma)t_0}}_{\to 0,1,\text{or}+\infty} + 3c_1\underbrace{\mathrm{e}^{(2-\gamma)t_0}}_{\to 0,1,\text{or}+\infty} + \underbrace{3c_1^2\mathrm{e}^{(1-\gamma)t_0}}_{\to+\infty} + \underbrace{c_1^3\mathrm{e}^{-\gamma t_0}}_{\to+\infty}.\end{aligned}$$

This confirms (4.20) and hence also $\lim_{t_0\to-\infty}\Phi_2(t_0) = 0$.

Consequently it follows that $\lim_{t_0\to-\infty}\frac{\varphi_2(t_0)}{\mathrm{e}^{-2\gamma t_0}} = 0$, $\lim_{t_0\to-\infty}\frac{\varphi(t_0)}{\mathrm{e}^{-2\gamma t_0}} = 0$, and finally $\lim_{t_0\to-\infty}\frac{a(t_0)}{b(t_0)} = 0$ what completes the proof.

□

Numerical Results

Numerical results in analogy to those of the linear model (Section 4.2) are shown in Figure 4.7. Here the Davis–Skodje test problem is used for computations with the *forward mode* (Fig. 4.7(a), 4.7(c)) and the *reverse mode* (Fig. 4.7(b), 4.7(d)). Here x_1 is the reaction progress variable (SIM parameterization) and fixed at several values between 0.2 and 2.0 for the computation of SIM points as solutions of the optimization problem. The spectral gap parameter is chosen as $\gamma = 1.2$ and $\gamma = 2.0$, respectively. The red curve represents the analytically calculated SIM $\mathcal{W}_\varepsilon = \{(x_1, x_2) \in \mathbb{R}^2 \mid x_2 = h_\varepsilon(x_1) = \frac{x_1}{1+x_1},\ x_1 \in K\}$, the blue curves are the trajectories integrated numerically from those points that are the solutions of the optimization problem (blue circles) and the red dot represents the chemical equilibrium point.

Forward mode solutions show a larger deviation from the SIM and lack invariance whereas *reverse mode* solutions are highly accurate representations of the SIM. Again the accuracy of approximation of the SIM improves with increasing time scale separation (i.e. with increasing γ). As in the linear case numerical solutions confirm the theoretical results.

In the following plot (Figure 4.8) the reaction progress variable $x_1^{t_\mathrm{f}}$ is fixed at $x_1^{t_\mathrm{f}} = 0.5$ and the optimization problem is solved for different values of γ by using always the same time interval $t_\mathrm{f} - t_0 = 7.5 \cdot 10^{-5}$. Then, $log(\gamma)$ is plotted against the logarithmic error $log(|h_\varepsilon(0.5) - x^*|)$ with $h_\varepsilon(0.5) = \frac{1}{3}$ ($x_2 = h_\varepsilon(x_1) = \frac{x_1}{x_1+1}$) and x^* being the optimal solution of the optimization problem (4.3) (using the Davis–Skodje model (4.14)).

In Figure 4.8 one can see that the approximation of the SIM $\mathcal{W}_\varepsilon = \{(x_1, x_2) \in \mathbb{R}^2 \mid x_2 = h_\varepsilon(x_1) = \frac{x_1}{1+x_1},\ x_1 \in K\}$ improves with increasing spectral gap parameter γ for $x_1^{t_\mathrm{f}} = 0.5$. Furthermore, the slope of the line through the points is ~ -2 what implicates the error $|h_\varepsilon(0.5) - x^*|$ being proportional to $\frac{1}{\gamma^2}$.

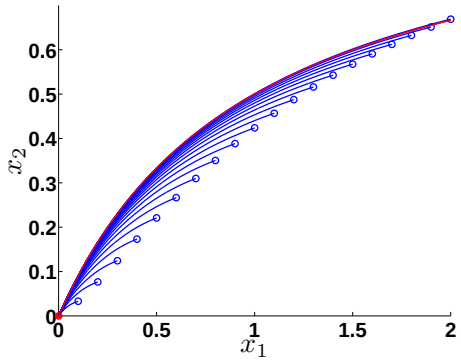

(a) *Forward mode*: $t_0 = 0.0$, $t_f = 10.0$, $\gamma = 1.2$.

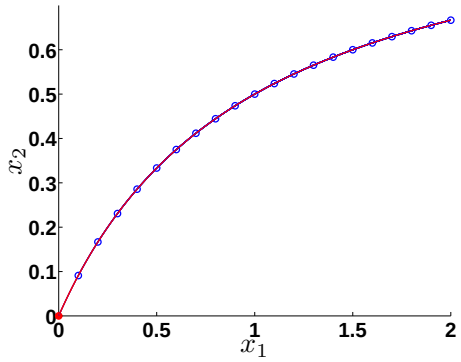

(b) *Reverse mode*: $t_0 = -8.0$, $t_f = 0.0$, $\gamma = 1.2$.

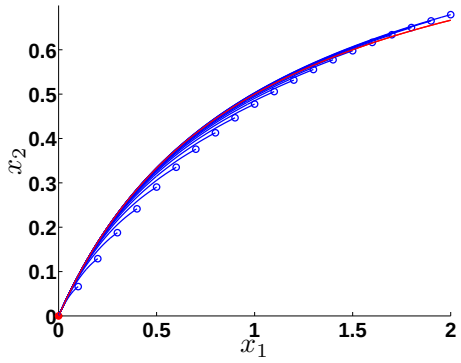

(c) *Forward mode*: $t_0 = 0.0$, $t_f = 10.0$, $\gamma = 2.0$.

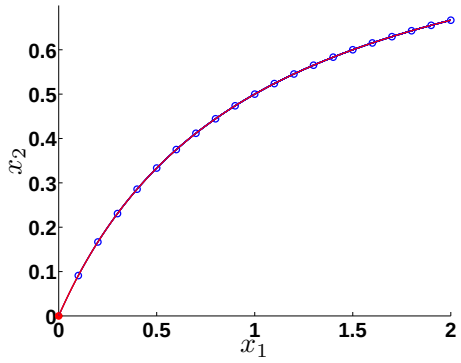

(d) *Reverse mode*: $t_0 = -8.0$, $t_f = 0.0$, $\gamma = 2.0$.

Figure 4.7: Results for the Davis–Skodje test problem with (a), (c) *forward mode*: $x_1(t_0) = x_1^{t_0}$, and (b), (d) *reverse mode*: $x_1(t_f) = x_1^{t_f}$. The spectral gap parameter is chosen as $\gamma = 1.2$ and $\gamma = 2.0$ respectively.

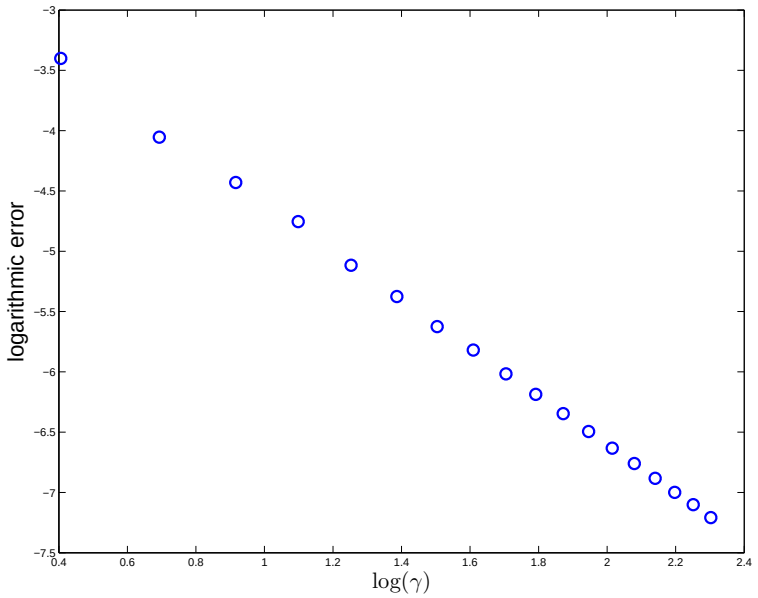

Figure 4.8: For different values of γ, $log(\gamma)$ is plotted against $log(|h_\varepsilon(0.5) - x^*|)$ for $x_1^{t_f} = 0.5$.

4.3.2 Semenov Model

Another two-dimensional non-linear test model is the Semenov model for thermal explosions [1, 2, 16, 35, 37] which is given by the following singular perturbation problem

$$\varepsilon \frac{\mathrm{d}x}{\mathrm{d}t} = \big(yq(x) - x\delta\big) \tag{4.21a}$$

$$\frac{\mathrm{d}y}{\mathrm{d}t} = -yq(x) \tag{4.21b}$$

with $q(x) = \exp\big(x/(1+\beta x)\big)$, $\delta = 1$, and $\beta = 0.31$. System (4.21) possesses a unique global SIM $\mathcal{W}_\varepsilon$ for $\varepsilon < 1$ with the equilibrium in the origin.

Figure 4.9 depicts numerical solution results of the optimization problem (4.3) with model (4.21) and two different values of ε. In contrast to the formulation (4.3) here the fast variable x is chosen as reaction progress variable in order to compare the results with the plots given in [2]. Figures 4.9(a) and 4.9(b) show that the approximation to the SIM is more accurate with decreasing ε (*forward mode*) what implicates an increasing time scale separation and Figures 4.9(c) and 4.9(d) demonstrate again that the approximation becomes better in the *reverse mode* formulation with increasing time interval. Obviously – comparing Figure 4.9(b) and Figure 4.9(d) – the *reverse mode* gives solutions that are significantly closer to the SIM (less inconsistent) than the solutions of the *forward mode*.

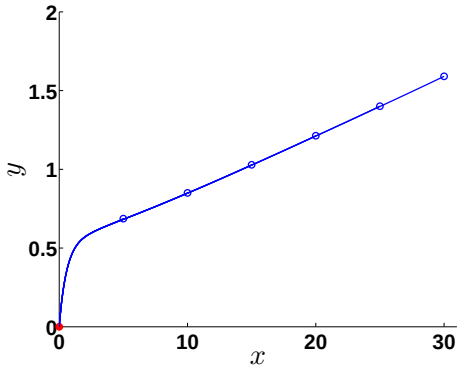

(a) *Forward mode*: $t_0 = 0.0$, $t_f = 10.0$, $\varepsilon = 10^{-3}$.

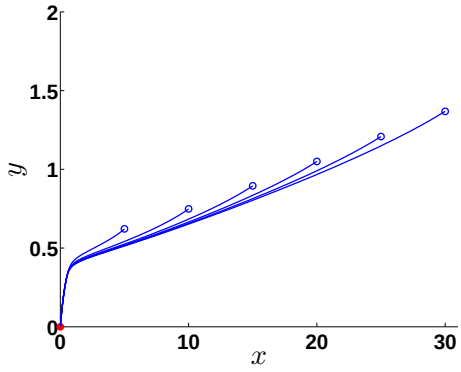

(b) *Forward mode*: $t_0 = 0.0$, $t_f = 10.0$, $\varepsilon = 10^{-2}$.

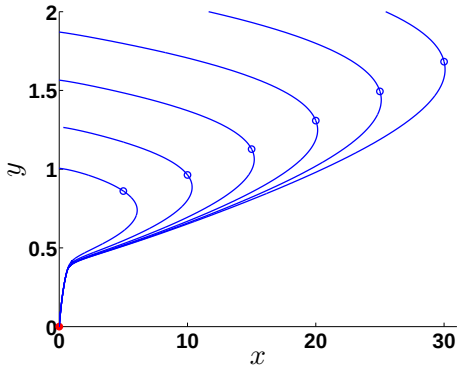

(c) *Reverse mode*: $t_0 = -0.04$, $t_f = 0.0$, $\varepsilon = 10^{-2}$.

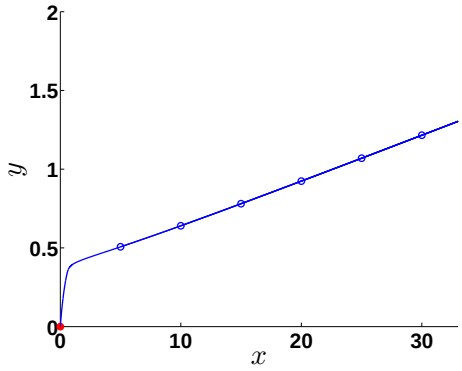

(d) *Reverse mode*: $t_0 = -0.4$, $t_f = 0.0$, $\varepsilon = 10^{-2}$.

Figure 4.9: Numerical solution results of the optimization problem (4.3) with model (4.21) (Semenov) and two different values of ε.

4.3.3 Model Hydrogen Combustion Reaction Mechanism

The first more realistic chemical mechanism used for the computations in this work is a six-species reaction mechanism without temperature dependency (see Table 3.1). The singular perturbed form of the corresponding ODE system is not known (note that it is assumed that there exists a diffeomorphism that transforms the ODE system into a singularly perturbed system) and this is why there is no accessible separation into fast and slow variables/species. The reaction progress variable is chosen more or less arbitrary (how to choose the reaction progress variable(s) depends on a detailed knowledge of chemical properties or on monotony properties of the parameterizing species along the SIM).

First numerical results for this mechanism are shown using the entropy production (3.2) as criterion in the optimization problem. Figure 4.10 depicts the solutions using the *forward mode* formulation whereas in Figure 4.11 the solutions of the

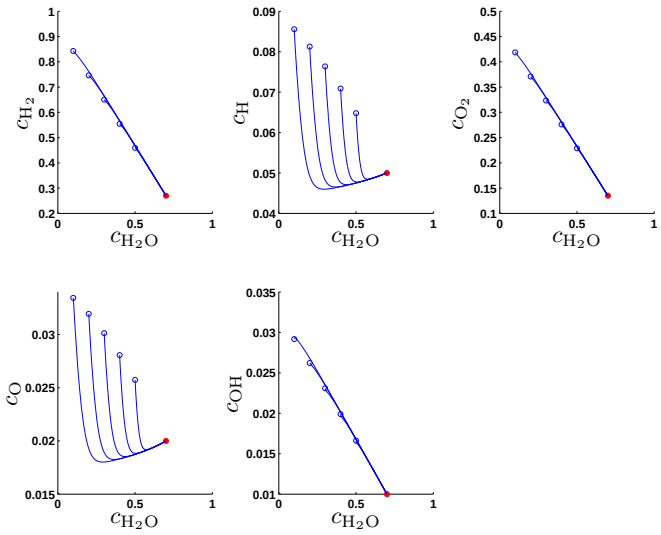

Figure 4.10: Numerical results for a 1-D SIM of the model hydrogen combustion reaction mechanism computed with the *forward mode* formulation and entropy production (3.2) as criterion. $t_0 = 0.0,\ t_f = 1.0$.

optimization problem including the *reverse mode* formulation are presented. In both cases c_{H_2O} is chosen as reaction progress variable and fixed at different values between 0.1 and 0.5. For a good visualization c_{H_2O} is plotted against the concentrations of the other (free) species in a way that the six-dimensional phase space can be visualized in five two-dimensional plots. Again the red dots represent the chemical equilibrium and the blue circles are the solution points of the optimization problem. The blue curves are the trajectories crossing the corresponding solution point. In subsequent figures this will always be the case if not otherwise stated.

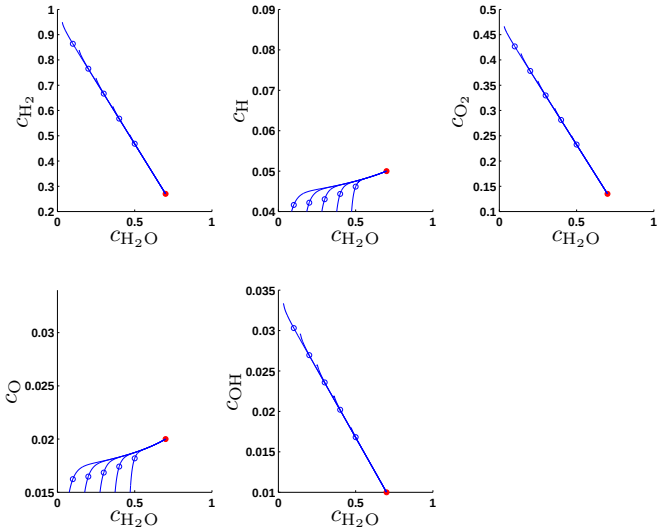

Figure 4.11: Numerical results for a 1-D SIM of the model hydrogen combustion reaction mechanism computed with the *reverse mode* formulation and entropy production (3.2) as criterion. $t_0 = -0.0305,\ t_\mathrm{f} = 0.0$.

As one can see the solutions of the *reverse mode* formulation are much closer to invariance than the solutions of the *forward mode* formulation but they are still fairly inconsistent.

As this criterion has fallen in disuse, the focus is now on the following one:

$$\Phi\left(c(t)\right) = \|J_f(c) \cdot f\|_2^2. \tag{4.22}$$

First, numerical results of the optimization problem including criterion (4.22) are shown using the *forward mode* formulation (Figure 4.12).

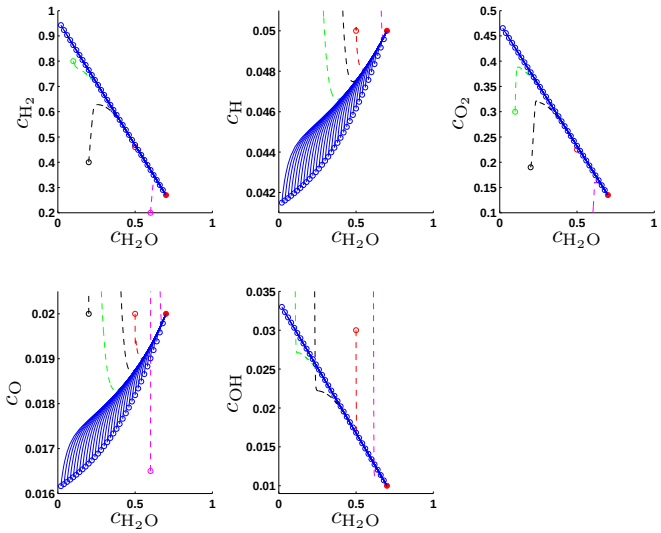

Figure 4.12: Numerical results for a 1-D SIM of the model hydrogen combustion reaction mechanism computed with *forward mode*, i.e. $c_{H_2O}(t_0) = c_{H_2O}^{t_0}$. $t_0 = 0.0$, $t_f = 1.0$. Arbitrary trajectories relax on the manifold (colored, dashed).

Here the reaction progress variable is fixed at different values between 0.01 and 0.65. The colored dashed curves are arbitrary trajectories starting from arbitrary initial values. These trajectories converge to the SIM and then stay close to it during convergence to chemical equilibrium. In comparison to Figure 3.3, where the same results are depicted with the difference that the Euclidean norm of the objective function is not squared (3.5) one can see that the solutions are nearly the same but still significantly inconsistent.

Now the results of the new *reverse mode* formulation are considered. Figure 4.13 shows the results of the optimization problem including this new formulation for a final time $t_\mathrm{f} = 0.0$ and an initial time of $t_0 = -0.001$.

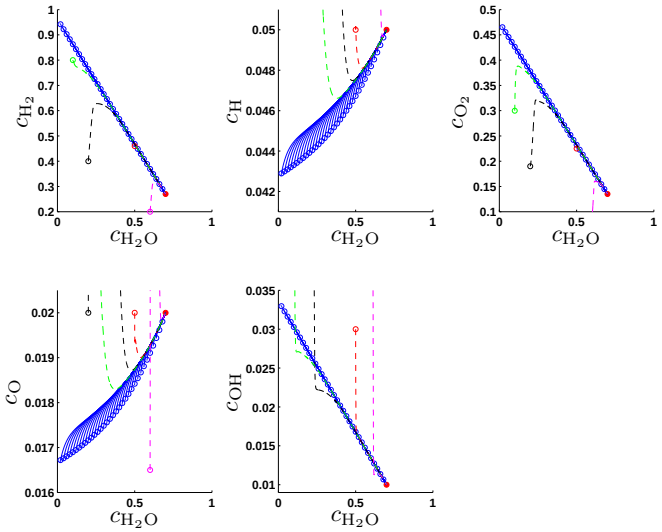

Figure 4.13: Numerical results for a 1-D SIM of the model hydrogen combustion reaction mechanism computed with *reverse mode*, i.e. $c_{\mathrm{H_2O}}(t_\mathrm{f}) = c^{t_\mathrm{f}}_{\mathrm{H_2O}}$. $t_0 = -0.001$, $t_\mathrm{f} = 0.0$. Arbitrary trajectories relax on the manifold (colored, dashed).

The solutions are less inconsistent than the results of the *forward mode* formulation (Figure 4.12).

By decreasing t_0 to $t_0 = -0.1$ the solutions show a decreasing inconsistency so that it seems that they characterize the SIM exactly. However it can also be seen that the trajectories starting from the solution points going backwards in time leave the SIM after a very short time which is caused by the fact that the solution points do not identify the SIM exactly.

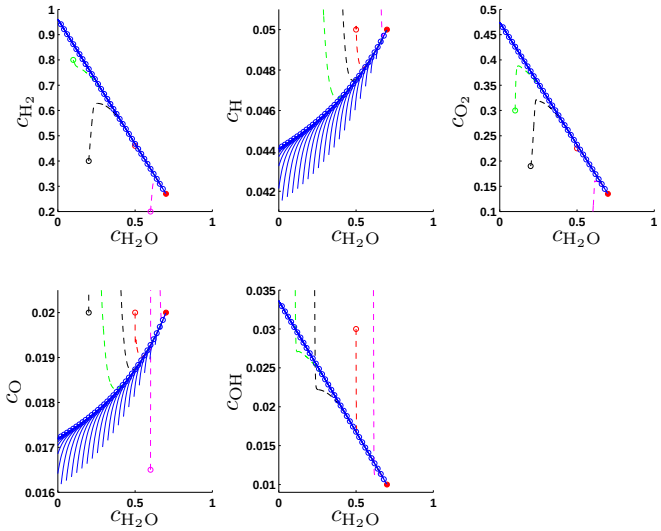

Figure 4.14: Numerical results for a 1-D SIM of the model hydrogen combustion reaction mechanism computed with *reverse mode*, i.e. $c_{H_2O}(t_f) = c^{t_f}_{H_2O}$. $t_0 = -0.1$, $t_f = 0.0$. Arbitrary trajectories relax on the manifold (colored, dashed).

If t_0 is chosen as $t_0 = -0.3$ it can be seen in Figure 4.15 that the trajectories going backwards in time from the solution points stay very close to the SIM for a longer time before they diverge from it. This means that the solution points characterized by blue circles are closer to the SIM than in the cases before.

In Figure 4.16 t_0 is decreased to $t_0 = -0.5$ and this implicates the solution points lying closer to the SIM. This can be seen by the trajectories going backwards in time.

Focusing on Figure 4.17 where t_0 is chosen as $t_0 = -0.75$ it can be supposed that the SIM is characterized exactly if an infinite time horizon is chosen ($t_f = 0$, $t_0 = -\infty$) as proved in the two-dimensional linear case and in the Davis–Skodje test model.

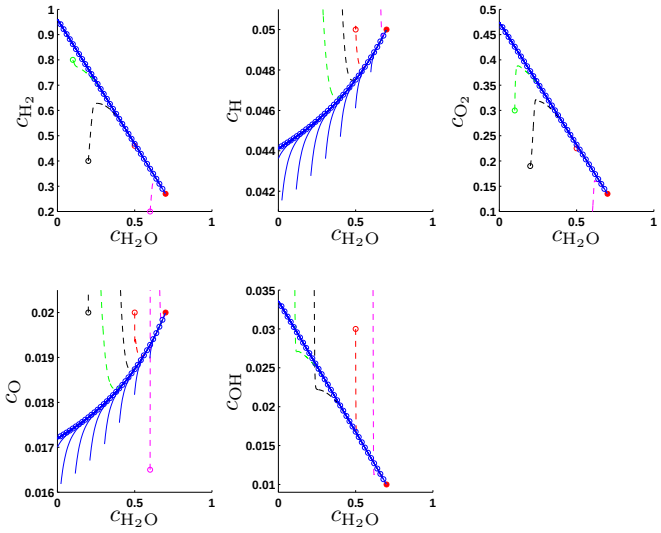

Figure 4.15: Numerical results for a 1-D SIM of the model hydrogen combustion reaction mechanism computed with *reverse mode*, i.e. $c_{\mathrm{H_2O}}(t_\mathrm{f}) = c^{t_\mathrm{f}}_{\mathrm{H_2O}}$. $t_0 = -0.3$, $t_\mathrm{f} = 0.0$. Arbitrary trajectories relax on the manifold (colored, dashed).

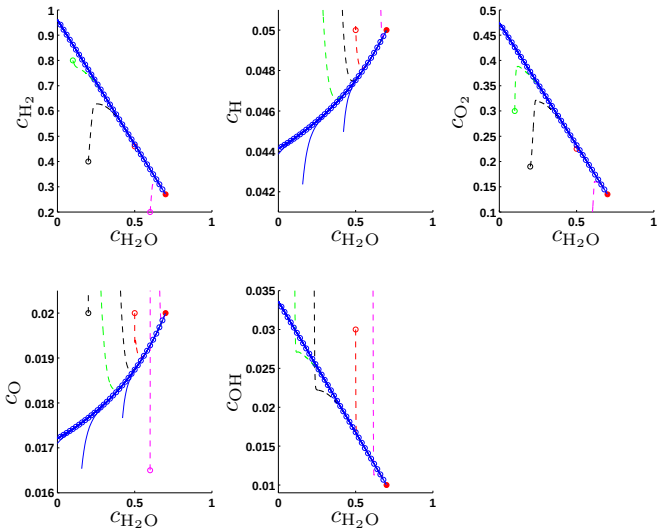

Figure 4.16: Numerical results for a 1-D SIM of the model hydrogen combustion reaction mechanism computed with *reverse mode*, i.e. $c_{\mathrm{H_2O}}(t_\mathrm{f}) = c^{t_\mathrm{f}}_{\mathrm{H_2O}}$. $t_0 = -0.5$, $t_\mathrm{f} = 0.0$. Arbitrary trajectories relax on the manifold (colored, dashed).

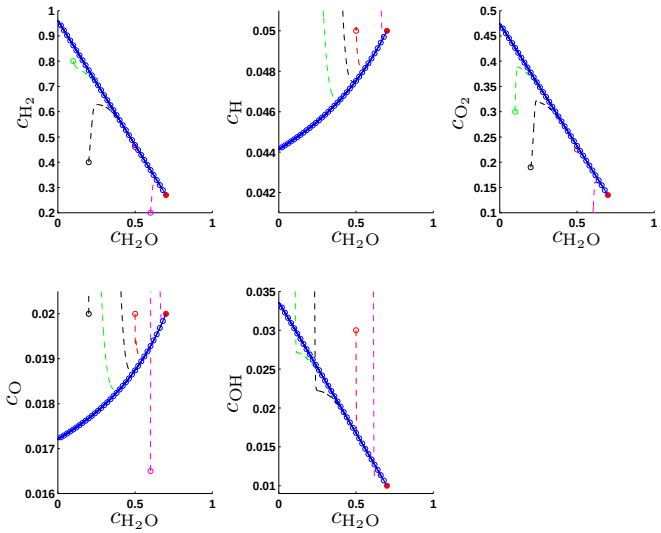

Figure 4.17: Numerical results for a 1-D SIM of the model hydrogen combustion reaction mechanism computed with *reverse mode*, i.e. $c_{H_2O}(t_f) = c^{t_f}_{H_2O}$. $t_0 = -0.75$, $t_f = 0.0$. Arbitrary trajectories relax on the manifold (colored, dashed).

As mentioned above this mechanism possesses four degrees of freedom. By fixing two variables as reaction progress variables there are still two degrees of freedom left for the optimization. This is why a two-dimensional manifold can also be computed. Figure 4.18 shows the results of a two-dimensional SIM computed with the *reverse mode* formulation and criterion (4.22). As reaction progress variables $c_{\mathrm{H_2O}}$ and $c_{\mathrm{H_2}}$ are chosen.

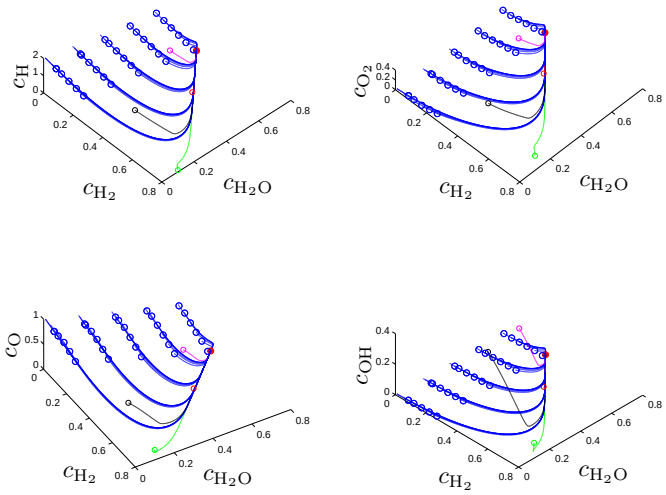

Figure 4.18: Numerical results for a 2-D SIM of the model hydrogen combustion reaction mechanism computed with *reverse mode*, i.e. $c_{\mathrm{H_2O}}(t_{\mathrm{f}}) = c^{t_{\mathrm{f}}}_{\mathrm{H_2O}}$, $c_{\mathrm{H_2}}(t_{\mathrm{f}}) = c^{t_{\mathrm{f}}}_{\mathrm{H_2}}$. $t_0 = -0.0001$, $t_{\mathrm{f}} = 0.0$. Arbitrary trajectories relax on the manifold (colored, dashed).

One point that can be seen in the three-dimensional plots is that the colored dashed curves, which are again arbitrary trajectories starting from arbitrary initial values, first converge to the two-dimensional and afterwards to the one-dimensional SIM during convergence to chemical equilibrium.

4.3.4 Simplified Realistic Mechanism

Numerical results for a simplified realistic (temperature dependent) mechanism for hydrogen combustion are presented. The corresponding full mechanism was originally published as a detailed hydrogen combustion mechanism by Li et al. in [29]. Ren et al. simplified the mechanism and used it for testing their ICE-PIC model reduction method in [34]. An adapted version of the simplified model is used here. It consists of six chemical species (including the inert gas N_2) and twelve chemical reactions as given in Table 4.1. Element mass conservation relations (equality constraints (4.3d)) for this mechanism are

$$\begin{aligned} c_{\mathrm{H}} + 2c_{\mathrm{H_2}} + c_{\mathrm{OH}} + 2c_{\mathrm{H_2O}} &= 0.15 \\ c_{\mathrm{OH}} + c_{\mathrm{O}} + c_{\mathrm{H_2O}} &= 0.05 \\ 2c_{\mathrm{N_2}} &= 1.6. \end{aligned}$$

Table 4.1: Simplified realistic mechanism including six species.

Reaction			A / cm, mol, s	b	E_a / $\frac{\mathrm{kJ}}{\mathrm{mol}}$
$\mathrm{O + H_2}$	$\rightarrow$	$\mathrm{H + OH}$	5.08×10^{04}	2.70	26.3
$\mathrm{H + OH}$	$\rightarrow$	$\mathrm{O + H_2}$	2.24×10^{04}	2.70	18.5
$\mathrm{H_2 + OH}$	$\rightarrow$	$\mathrm{H_2O + H}$	2.16×10^{08}	1.50	14.4
$\mathrm{H_2O + H}$	$\rightarrow$	$\mathrm{H_2 + OH}$	9.62×10^{08}	1.50	77.7
$\mathrm{O + H_2O}$	$\rightarrow$	$\mathrm{2\,OH}$	2.97×10^{06}	2.00	56.1
$\mathrm{2\,OH}$	$\rightarrow$	$\mathrm{O + H_2O}$	2.94×10^{05}	2.00	−15.1
$\mathrm{H_2 + M}$	$\rightarrow$	$\mathrm{2\,H + M}$	4.58×10^{19}	−1.40	436.7
$\mathrm{2\,H + M}$	$\rightarrow$	$\mathrm{H_2 + M}$	1.18×10^{19}	−1.40	0.7
$\mathrm{O + H + M}$	$\rightarrow$	$\mathrm{OH + M}$	4.71×10^{18}	−1.00	0.0
$\mathrm{OH + M}$	$\rightarrow$	$\mathrm{O + H + M}$	8.07×10^{18}	−1.00	428.2
$\mathrm{H + OH + M}$	$\rightarrow$	$\mathrm{H_2O + M}$	3.80×10^{22}	−2.00	0.0
$\mathrm{H_2O + M}$	$\rightarrow$	$\mathrm{H + OH + M}$	6.57×10^{23}	−2.00	499.4

The reaction rates k_+ and k_- can be computed by the *Arrhenius law*

$$k = AT^b \exp\left(-\frac{E_\mathrm{a}}{RT}\right)$$

where T is the temperature (here fixed at 3000K) and R is the gas constant ($R = 8.314472\ \mathrm{J/(K \cdot mol)}$).

The corresponding ODE system can be written as:

$$
\begin{aligned}
\frac{\mathrm{d}c_{\mathrm{H}}}{\mathrm{d}t} = &+ k_1 c_{\mathrm{H_2}} c_{\mathrm{O}} && - k_{-1} c_{\mathrm{H}} c_{\mathrm{OH}} \\
&+ k_2 c_{\mathrm{H_2}} c_{\mathrm{OH}} && - k_{-2} c_{\mathrm{H}} c_{\mathrm{H_2O}} \\
&+ 2k_4 c_{\mathrm{H_2}} M_0 && - 2k_{-4} c_{\mathrm{H}}^2 M_0 \\
&- k_5 c_{\mathrm{H}} c_{\mathrm{O}} M_0 && + k_{-5} c_{\mathrm{OH}} M_0 \\
&- k_6 c_{\mathrm{H}} c_{\mathrm{OH}} M_0 && + k_{-6} c_{\mathrm{H_2O}} M_0 \\
\frac{\mathrm{d}c_{\mathrm{H_2}}}{\mathrm{d}t} = &- k_1 c_{\mathrm{H_2}} c_{\mathrm{O}} && + k_{-1} c_{\mathrm{H}} c_{\mathrm{OH}} \\
&- k_2 c_{\mathrm{H_2}} c_{\mathrm{OH}} && + k_{-2} c_{\mathrm{H}} c_{\mathrm{H_2O}} \\
&- 2k_4 c_{\mathrm{H_2}} M_0 && + 2k_{-4} c_{\mathrm{H}}^2 M_0 \\
\frac{\mathrm{d}c_{\mathrm{OH}}}{\mathrm{d}t} = &+ k_1 c_{\mathrm{H_2}} c_{\mathrm{O}} && - k_{-1} c_{\mathrm{H}} c_{\mathrm{OH}} \\
&- k_2 c_{\mathrm{H_2}} c_{\mathrm{OH}} && + k_{-2} c_{\mathrm{H}} c_{\mathrm{H_2O}} \\
&+ 2k_3 c_{\mathrm{O}} c_{\mathrm{H_2O}} && - 2k_{-3} c_{\mathrm{OH}}^2 \\
&+ k_5 c_{\mathrm{H}} c_{\mathrm{O}} M_0 && - k_{-5} c_{\mathrm{OH}} M_0 \\
&- k_6 c_{\mathrm{H}} c_{\mathrm{OH}} M_0 && + k_{-6} c_{\mathrm{H_2O}} M_0 \\
\frac{\mathrm{d}c_{\mathrm{O}}}{\mathrm{d}t} = &- k_1 c_{\mathrm{H_2}} c_{\mathrm{O}} && + k_{-1} c_{\mathrm{H}} c_{\mathrm{OH}} \\
&- k_3 c_{\mathrm{O}} c_{\mathrm{H_2O}} && + k_{-3} c_{\mathrm{OH}}^2 \\
&- k_5 c_{\mathrm{H}} c_{\mathrm{O}} M_0 && + k_{-5} c_{\mathrm{OH}} M_0 \\
\frac{\mathrm{d}c_{\mathrm{H_2O}}}{\mathrm{d}t} = &+ k_2 c_{\mathrm{H_2}} c_{\mathrm{OH}} && - k_{-2} c_{\mathrm{H}} c_{\mathrm{H_2O}} \\
&- k_3 c_{\mathrm{O}} c_{\mathrm{H_2O}} && + k_{-3} c_{\mathrm{OH}}^2 \\
&+ k_6 c_{\mathrm{H}} c_{\mathrm{OH}} M_0 && - k_{-6} c_{\mathrm{H_2O}} M_0 \\
\frac{\mathrm{d}c_{\mathrm{N_2}}}{\mathrm{d}t} = &\ 0
\end{aligned}
$$

with

$$M_0 = c_{\mathrm{H}} + 2.5 c_{\mathrm{H_2}} + c_{\mathrm{OH}} + c_{\mathrm{O}} + 12 c_{\mathrm{H_2O}} + c_{\mathrm{N_2}}.$$

Since a diffeomorphism that transforms the ODE system above in a singular perturbed form is not known, the choice of the reaction progress variable is again more or less arbitrarily $c_{\mathrm{H_2O}}$.

In Figures 4.19 and 4.20 results for the computation of a one-dimensional SIM for the hydrogen combustion mechanism are shown. Solutions of the optimization problem (4.3) have been computed using the *forward mode* formulation and the *reverse mode* formulation, respectively. The progress variable $c_{\mathrm{H_2O}}$ has been fixed at different values between 0.0005 and 0.0180. Both *forward mode* and *reverse mode* accurately approximate the SIM. Convergence of trajectories (dashed red curves) started from arbitrary initial values (red circles) to the computed SIM is visualized in Figures 4.19 and 4.20.

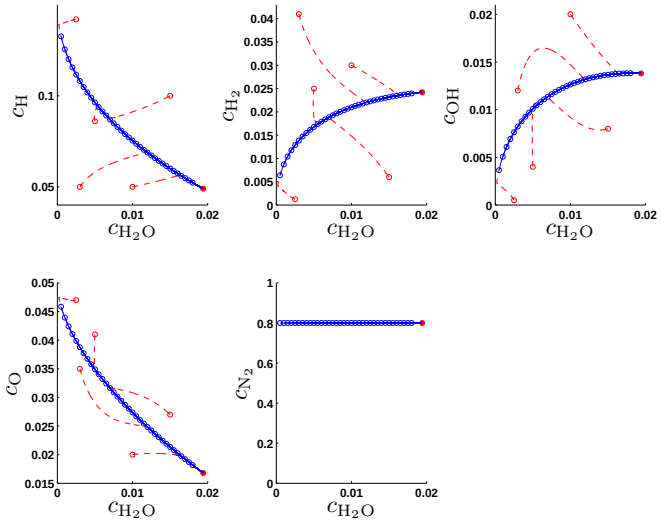

Figure 4.19: Numerical results for a 1-D SIM of the simplified combustion mechanism computed with *forward mode*, i.e. $c_{\mathrm{H_2O}}(t_0) = c^{t_0}_{\mathrm{H_2O}}$. $t_0 = 0.0$, $t_{\mathrm{f}} = 0.1$, temperature $T = 3000$ K. Arbitrary trajectories relax on the manifold (red, dashed).

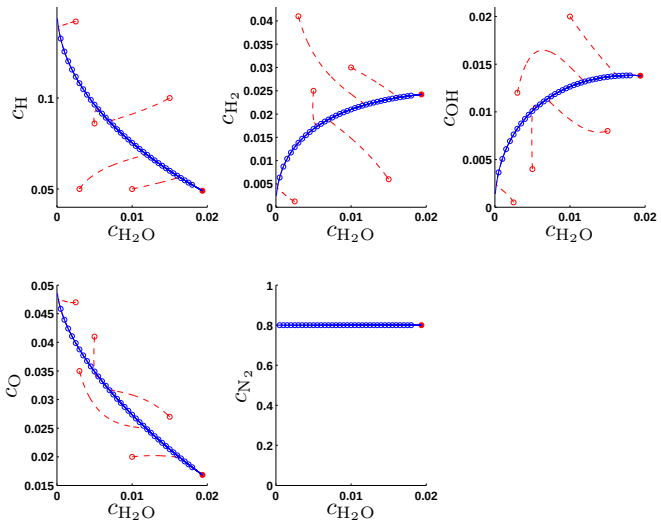

Figure 4.20: Numerical results for a 1-D SIM of the simplified combustion mechanism computed with *reverse mode*, i.e. $c_{\mathrm{H_2O}}(t_\mathrm{f}) = c^{t_\mathrm{f}}_{\mathrm{H_2O}}$. $t_0 = -0.0004$, $t_\mathrm{f} = 0.0$, temperature $T = 3000$ K. Arbitrary trajectories relax on the manifold (red, dashed).

Figure 4.21 shows a two-dimensional manifold computed with the *reverse mode*. The reaction progress variables c_{H_2O} and c_{H_2} are fixed and the SIM is approximated on a two-dimensional grid as a solution of a family of optimization problems. The computation of the two-dimensional manifold is possible because the mechanism contains six species, three conservation equalities, and two fixed variables (progress variables). Hence there is still one degree of freedom left for the optimization.

Again convergence of trajectories (red curves) started from arbitrary initial values (red circles) to the computed SIM is observed.

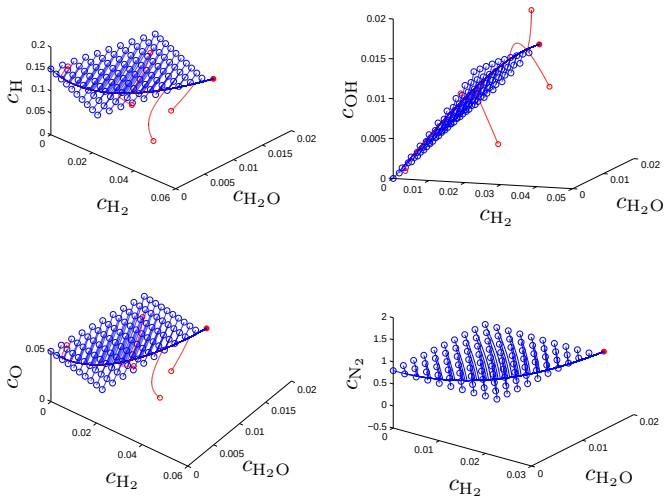

Figure 4.21: Numerical results for a 2-D SIM of the simplified combustion mechanism computed with *reverse mode* and $c_{H_2O}(t_f)$ and $c_{H_2}(t_f)$ chosen as reaction progress variables, $t_0 = -5.0\times10^{-7}$, $t_f = 0.0$, constant temperature $T = 3000$ K. The same arbitrary trajectories as in Fig. 4.20 are shown in red.

Chapter 5

Summary and Outlook

5.1 Summary

Model reduction techniques have to be applied because it is computationally highly expensive – despite growing computing power – to solve reactive flow simulation including large reaction mechanisms consisting of hundreds of species and reactions. These reaction mechanisms can be described by systems of *Ordinary Differential Equations (ODEs)*. Model reduction approaches aim at a description of the full reaction mechanism in a low-dimensional approximation via eliminating the fast modes of the system by enslaving them to the slow ones. If *Slow Invariant attracting Manifolds (SIMs)* are present in the phase space of the dynamical system, most reduction methods try to identify and approximate those SIMs, whose dynamics govern the long term dynamics of the full model. It follows that the full model can be reduced via approximating these SIMs. One of these model reduction approaches via SIM computation is the *trajectory-based optimization approach*, which is analyzed in this thesis.

Lebiedz formulated an optimization approach for approximating SIMs in 2004 [22], where the *entropy production rate* was used as criterion in the objective function. Later other criteria have been developed involving the curvature of the state vector. The constraints of the optimization problem include the system dynamics (model equations) described by an ODE system, the fixation of specified variables that parameterize the SIM at a specified point of time, and additional constraints (e.g. mass conservation equations in chemical kinetics). These parameterizing variables – naturally the slow variables of the system – are called *reaction progress variables*. For the determination of a point of the SIM, *species reconstruction* is used, which represents a function mapping such reaction progress variables onto the full species composition by determining a point on the SIM.

In this work a new formulation of the optimization approach called *reverse mode* is presented. The basic idea of this approach goes back to Dirk Lebiedz. In this formulation the reaction progress variables are not fixed at the initial point of time t_0 (*forward mode*) but at the final point of time t_f. Thus, more information of the trajectory can be taken into account by decreasing t_0. Numerical solutions show a very good performance. Also analytical results are stated where it is shown for a two-dimensional linear mechanism and the non-linear Davis–Skodje problem (4.14) that solutions of the *reverse mode* characterize the SIM exactly for an infinite time horizon of the optimization problem. These analytical results achieved with the new *reverse mode* formulation are the central parts of this thesis. For numerical computations a code – developed by Jochen Siehr – has been adapted to the mechanisms.

5.2 Outlook

The main tasks of the project in future can be divided into two parts:

- First the application to large-scale mechanisms including dozens or even hundreds of species.

- The second point is the extension of analytical results to the general linear and non-linear case at a singularly perturbed system.

5.2.1 Application to Large-Scale Mechanisms

In order to apply the presented model reduction method to realistic large-scale mechanisms the number of state variables of the used mechanisms has to be increased rapidly. In this work chemical mechanisms including six species are analyzed. As a first step a mechanism including nine species is already applied but there are still problems by using the *reverse mode*. In contrast to this the mechanism works stable by using the *forward mode* formulation.

Chemical mechanisms involve varying temperature while the reaction takes place. Since the temperature is constant up to now additional constraints should be added to the optimization problem in a way that the temperature can vary. Also other physical aspects like pressure have to be regarded.

Another issue to apply large-scale mechanisms is the necessity of decreasing the computing time via upgrading the code that is used for solving the optimization problem.

5.2.2 Extension of Analytical Results

A further focal point is the continuation of analytical calculations. As a first step it is stated in this thesis that the solutions of the *reverse mode* formulation characterize the SIM exactly for an infinite time horizon by using two simple test problems. These results should be extended to the general linear case

$$\dot{c}(t) = Ac(t), \quad c(t) \in \mathbb{R}^n,\ A \in \mathbb{R}^{n \times n}$$

where A is a matrix with eigenvalues $-\lambda,\ -\lambda - \gamma_1, \ldots, -\lambda - \gamma_{n-1}$ with $\lambda, \gamma_i \geqslant 0,\ i = 1, \ldots, n-1$ and if possible to the general non-linear case

$$\dot{c}(t) = f\left(c(t)\right),\ c(t) \in \mathbb{R}^n.$$

Furthermore there is a similarity to the Zero Derivative Principle (ZDP) (see Section 1.2). First analysis of the linear mechanism (4.6) show that results improve for an increasing derivation of the state vector in the objective function, i.e.

$$\int_{t_0}^{t_\mathrm{f}} \Phi\left(c(t)\right)\ \mathrm{d}t = \int_{t_0}^{t_\mathrm{f}} \left\| \frac{\mathrm{d}^n c}{\mathrm{d}t^n} \right\|_2^2 \mathrm{d}t, \quad n > 0.$$

This suggests a relation between the presented trajectory-based model reduction method and the ZDP.

Bibliography

[1] A. Adrover, F. Creta, S. Cerbelli, M. Valorani, and M. Giona. "The structure of slow invariant manifolds and their bifurcational routes in chemical kinetic models". *Computers and Chemical Engineering*, vol. 31, pp. 1456–1474, 2007.

[2] A. Adrover, F. Creta, M. Giona, and M. Valorani. "Stretching-based diagnostics and reduction of chemical kinetic models with diffusion". *Journal of Computational Physics*, vol. 225, pp. 1442–1471, 2007.

[3] P. Atkins and J. de Paula. *Physical Chemistry.* Oxford University Press, eighth edn., 2006.

[4] B. M. Bell and J. V. Burke. "Algorithmic differentiation of implicit functions and optimal values". In C. H. Bischof, H. M. Bücker, P. D. Hovland, U. Naumann, and J. Utke, eds., "Advances in automatic differentiation", pp. 67–77. Springer, 2008.

[5] M. Bodenstein. "Eine Theorie der photochemische Reaktionsgeschwindigkeiten". *Zeitschrift für Physikalische Chemie – Leipzig*, vol. 85, pp. 329–397, 1913.

[6] M. Bodenstein and H. Lütkemeyer. "Die photochemische Bildung von Bromwasserstoff und die Bildungsgeschwindigkeit der Brommolekel aus den Atomen". *Zeitschrift für Physikalische Chemie*, vol. 114, pp. 208–236, 1924.

[7] D. L. Chapman and L. K. Underhill. "The interaction of chlorine and hydrogen. The influence of mass." *Journal of the Chemical Society, Transactions*, vol. 103, pp. 496–508, 1913.

[8] M. J. Davis and R. T. Skodje. "Geometric investigation of low-dimensional manifolds in systems approaching equilibrium". *Journal of Chemical Physics*, vol. 111, pp. 859–874, 1999.

[9] P. Deuflhard and F. Bornemann. *Numerische Mathematik II.* Walter de Gruyter, New York, second edn., 2002.

[10] N. Fenichel. "Persistence and smoothness of invariant manifolds for flows". *Indiana University Mathematics Journal*, vol. 21, pp. 193–226, 1972.

[11] N. Fenichel. "Asymptotic stability with rate conditions". *Indiana University Mathematics Journal*, vol. 23, pp. 1109–1137, 1974.

[12] N. Fenichel. "Asymptotic Stability with Rate Conditions II". *Indiana University Mathematics Journal*, vol. 26, pp. 81–93, 1977.

[13] N. Fenichel. "Geometric singular perturbation theory for ordinary differential equations". *Journal of Differential Equations*, vol. 31, pp. 53–98, 1979.

[14] R. Fletcher and S. Leyffer. "Nonlinear programming without a penalty function". *Mathematical Programming*, vol. 91, pp. 239–269, 2002.

[15] C. W. Gear, T. J. Kaper, I. G. Kevrekidis, and A. Zagaris. "Projecting to a Slow Manifold: Singularly Perturbed Systems and Legacy Codes". *SIAM Journal on Applied Dynamical Systems*, vol. 4, pp. 711–732, 2005.

[16] I. Goldfarb, V. Gol'dshtein, and U. Maas. "Comparative analysis of two asymptotic approaches based on integral manifolds". *IMA Journal of Applied Mathematics*, vol. 69, pp. 353–374, 2004.

[17] A. N. Gorban, I. V. Karlin, and A. Y. Zinovyev. "Constructive methods of invariant manifolds for kinetic problems". *Physics Reports*, vol. 396, pp. 197–403, 2004.

[18] J. Guckenheimer and P. Holmes. *Nonlinear oscillations, dynamical systems, and bifurcations of vector fields*. No. 42 in Applied Mathematical Sciences, Springer, New York, fifth edn., 1997.

[19] HSL. "A Collection of Fortran codes for large-scale scientific computation.", 2007. URL `http://www.hsl.rl.ac.uk`.

[20] C. K. R. T. Jones. "Geometric Singular Perturbation Theory". In R. Johnson, ed., "Dynamical Systems", chap. 2, pp. 44–118. No. 1609 in Lecture Notes in Mathematics, Springer, Heidelberg, 1995.

[21] T. J. Kaper. "An introduction to geometric methods and dynamical systems theory for singular perturbation problems". In J. Cronin, ed., "Analyzing multiscale phenomena using singular perturbation methods", *Proceedings of Symposia in Applied Mathematics*, vol. 56, pp. 85–124. American Mathematical Society, Providence, RI, 1999.

[22] D. Lebiedz. "Computing minimal entropy production trajectories: An approach to model reduction in chemical kinetics". *Journal of Chemical Physics*, vol. 120, pp. 6890–6897, 2004.

[23] D. Lebiedz. "Optimal control, model- and complexity-reduction of self-organized chemical and biochemical systems: A scientific computing approach". Habilitation thesis, University of Heidelberg, 2006.

[24] D. Lebiedz. "Entropy-related extremum principles for model reduction of dynamical systems". *Entropy*, vol. 12, pp. 706–719, 2010.

[25] D. Lebiedz, V. Reinhardt, and J. Kammerer. "Novel trajectory based concepts for model and complexity reduction in (bio)chemical kinetics". In A. N. Gorban, N. Kazantzis, I. G. Kevrekidis, and C. Theodoropoulos, eds., "Model reduction and coarse-graining approaches for multi-scale phenomena", pp. 343–364. Springer, Berlin, 2006.

[26] D. Lebiedz, V. Reinhardt, and J. Siehr. "Minimal curvature trajectories: Riemannian geometry concepts for slow manifold computation in chemical kinetics". *Journal of Computational Physics*, vol. 229, pp. 6512–6533, 2010.

[27] D. Lebiedz, J. Siehr, and J. Unger. "A variational principle for computing slow invariant manifolds in dissipative dynamical systems". arXiv:0912.1297, 2010.

[28] D. Lebiedz, D. Skanda, and M. Fein. "Automatic complexity analysis and model reduction of nonlinear biochemical systems". In "Computational methods in systems biology", pp. 123–140. Springer, 2008.

[29] J. Li, Z. Zhao, A. Kazakov, and F. L. Dryer. "An updated comprehensive kinetic model of hydrogen combustion". *International Journal of Chemical Kinetics*, vol. 36, pp. 566–575, 2004.

[30] L. Michaelis and M. L. Menten. "Die Kinetik der Invertinwirkung". *Biochemische Zeitschrift*, vol. 49, pp. 333–369, 1913.

[31] J. Nocedal and S. J. Wright. *Numerical Optimization*. Springer Series in Operations Research and Financial Engineering, Springer, New York, second edn., 2006.

[32] V. Reinhardt. "On the application of trajectory-based optimization for nonlinear kinetic model reduction". Ph.D. thesis, University of Heidelberg, 2008.

[33] V. Reinhardt, M. Winckler, and D. Lebiedz. "Approximation of slow attracting manifolds in chemical kinetics by trajectory-based optimization approaches". *Journal of Physical Chemistry A*, vol. 112, pp. 1712–1718, 2008.

[34] Z. Ren, S. B. Pope, A. Vladimirsky, and J. M. Guckenheimer. "The invariant constrained equilibrium edge preimage curve method for the dimension reduction of chemical kinetics". *Journal of Chemical Physics*, vol. 124, p. 114 111, 2006.

[35] N. N. Semenov. "Zur Theorie des Verbrennungsprozesses". *Zeitschrift für Physik A Hadrons and Nuclei*, vol. 48, pp. 571–582, 1928.

[36] S. Singh, J. M. Powers, and S. Paolucci. "On slow manifolds of chemically reactive systems". *Journal of Chemical Physics*, vol. 117, pp. 1482–1496, 2002.

[37] A. Varma, M. Morbidelli, and H. Wu. *Parametric Sensitivity In Chemical Systems*. Cambridge University Press, 1999.

[38] A. Wächter and L. T. Biegler. "Line search filter methods for nonlinear programming: Motivation and global convergence". *SIAM Journal on Optimization*, vol. 16, pp. 1–31, 2005.

[39] A. Wächter and L. T. Biegler. "On the implementation of a primal-dual interior point filter line Search Algorithm for Large-Scale Nonlinear Programming". *Mathematical Programming*, vol. 106, pp. 25–57, 2006.

[40] W. Walter. *Gewöhnliche Differentialgleichungen*. Springer, Berlin, sixth edn., 1996.

[41] J. Warnatz, U. Maas, and R. W. Dibble. *Combustion: Physical and Chemical Fundamentals, Modeling and Simulation, Experiments, Pollutant Formation*. Springer, Berlin, 2006.

[42] S. Wiggins. *Introduction to Applied Nonlinear Dynamical Systems and Chaos*. No. 2 in Texts in Applied Mathematics, Springer, New York, third edn., 1996.

[43] M. Winckler. "Towards optimal criteria for trajectory-based model reduction in chemical kinetics via numerical optimization". Diploma thesis, University of Heidelberg, 2007.

[44] A. Zagaris, C. W. Gear, T. J. Kaper, and Y. G. Kevrekidis. "Analysis of the accuracy and convergence of equation-free projection to a slow manifold". *ESAIM: Mathematical Modelling and Numerical Analysis*, vol. 43, pp. 757–784, 2009.